2. Materials and methods

2.1. Animals

Male C57/BL6J mice weighing 25–30 g (8–14 weeks old) were housed in a temperature (25 ± 2 °C)- and moisture (50%)-controlled room with a 12 h light/dark cycle (6:00 AM/6:00 PM). The mice were fed standard mouse chow (Oriental Yeast, Osaka) and tap water *ad libitium*, and used as wild-type mice.

Generation of GIPR$^{-/-}$ mice and GLP-1 receptor-deficient mice (GLP-1R$^{-/-}$ mice) was described previously [2,6]. GLP-1R$^{-/-}$ mice were kindly provided by Dr. Daniel J. Drucker [6]. Age-matched male GIPR$^{-/-}$ and GLP-1R$^{-/-}$ mice were used in the experiments. The Animal Care Committee of Kyoto University Graduate School of Medicine approved animal care and procedures.

2.2. Materials

Synthetic human GIP was purchased from Peptide Institute (Osaka, Japan). The somatostatin receptor antagonist, cyclo(7-aminoheptanoyl-PHE-$_D$-TRP-LYS-THR(BZL)) (cyclosomatostatin (CSS)) and somatostatin 28 (SST) were from Sigma Chemical Co. (St. Louis, MO). All other chemicals were of reagent grade.

2.3. Perfusion experiment

Single-pass perfusion method [7] was used to measure the effect of exogenous GIP or SST on intestinal glucose absorption using C57/BL6J mice. Preperfusion was done for a 45 min equilibration period and the samples were discarded. Three 15 min samples were then collected. GIP or SST was administered intraperitoneally at 60 min after starting the preperfusion according to the protocol (Fig. 1A). The change of absorption was calculated as the glucose concentration of the first sample collected (Period 1) minus the glucose concentration of the last sample collected (Period 2), and expressed as per centimeter perfused bowel. Negative values indicate an inhibitory effect on absorption; positive values indicate an increased effect on absorption.

2.4. Glucose uptake in jejunum in vitro

Incorporation of D-glucose into everted jejunal rings was determined as described previously [8]. SGLT-dependent glucose uptake for 15 min was determined as the glucose uptake in the absence of phlorizin minus the glucose uptake in the presence of phlorizin.

2.5. Small intestinal transit after intraperitoneal administration of GIP

Transit through the stomach and small intestine was measured by administering a non-absorbed marker containing 10% charcoal suspension in 5% gum Arabic, as previously described [9]. The mice were given 0.2 ml of the suspension by gavage through a straight blunt-ended feeding needle. GIP (50 nmol/kg body weight) or SST (75 nmol/kg body weight) or vehicle (saline) was administered intraperitoneally 15 min prior to the administration of the non-absorbed marker. CSS (1 μg/kg body weight), or vehicle (saline) was intraperitoneally administered 10 min prior to GIP administration.

2.6. Plasma GIP and SST assays

Blood was collected from the tail vein before the intraperitoneal administration of GIP (50 nmol/kg body weight) and collected again 20 min after the administration. ELISA assay kit was used according to the manufacture's instruction for the determination of plasma total GIP concentration (Linco Research, St. Charles, MO) and SST concentration (Phoenix Pharmaceuticals INC., Belmont, CA), respectively.

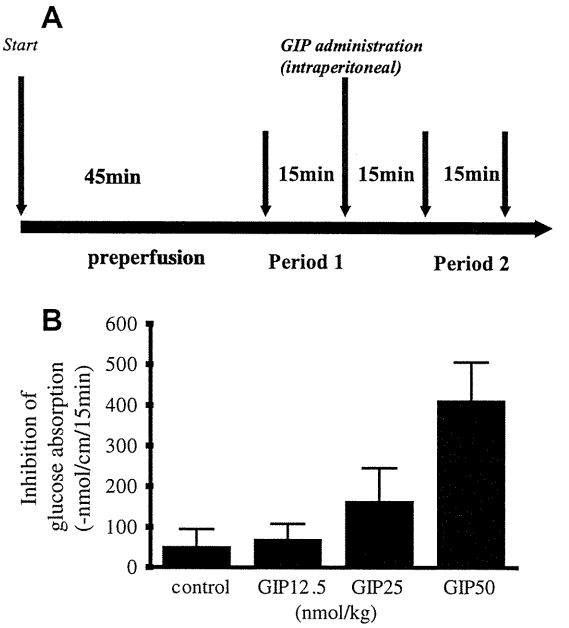

Fig. 1. (A) Diagram showing the sampling protocol of intestinal perfusion. The flow rate of the perfusion fluid was 2 ml/15 min. Perfusion began with an equilibration period of 45 min, which samples were discarded. The samples of Period 1 and Period 2 were then collected. GIP was administered intraperitoneally 60 min after the beginning of preperfusion. The change of absorption was calculated as the glucose concentration of the first samples collected (Period 1) minus the glucose concentration of the last samples collected (Period 2), and expressed as per centimeter perfused bowel. (B) Concentration-dependence of inhibition of glucose absorption by GIP in wild-type mice. Data are shown as means with SEM ($n = 6$ for each group, $P < 0.05$ by ANOVA).

2.7. Analysis

The results are given as mean ± standard error (SEM, n = number of mice). Statistical significance was determined using paired and unpaired Student's t-test and analysis of variance (ANOVA). $P < 0.05$ was considered significant.

3. Results

3.1. Perfusion experiment

Inhibition of glucose absorption was calculated by change in glucose concentration in effluent perfusate in wild-type mice (Fig. 1A). Spontaneous inhibition of glucose absorption of 49 ± 44 nmol/cm/15 min is shown in saline-administered controls (Fig. 1B). Inhibition of glucose absorption was enhanced to 67 ± 40, 163 ± 84, and 409 ± 96 nmol/cm/15 min when the amount of intraperitoneally-administered GIP was increased to 12.5, 25, and 50 nmol/kg body weight, respectively.

3.2. Glucose uptake by jejunum in vitro

We investigated glucose uptake by the jejunum *in vitro* using everted jejunal rings. In the presence of 100 nM GIP in the incubation medium, glucose uptake into jejunal rings in wild-type mice was similar to that in the presence of vehicle (control: 4.2 ± 0.9 μmol/g weight; GIP: 3.5 ± 0.9, P = NS; Fig. 2A). Additionally, glucose uptake into jejunal rings in GIPR$^{-/-}$ mice was similar

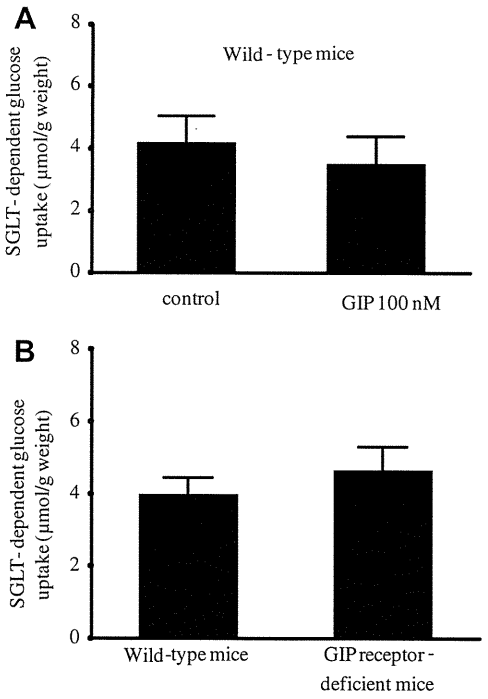

Fig. 2. Glucose uptake in the jejunum. (A) Glucose uptake in the jejunum in wild-type mice in the absence and in the presence of 100 nM GIP. (B) Glucose uptake in the jejunum in wild-type and GIPR$^{-/-}$ mice. SGLT-dependent glucose uptake was determined as the glucose uptake in the absence of 1 mM phlorizin minus the glucose uptake in the presence of 1 mM phlorizin. Data are shown as means with SEM ($n = 8$ for each group).

to that in wild-type mice (wild-type mice: 4.0 ± 0.5 μmol/g weight; GIPR$^{-/-}$ mice 4.6 ± 0.7, P = NS; Fig. 2B).

3.3. Small intestinal transit after intraperitoneal administration of GIP

Intestinal transit rate was measured by the length of small intestine traversed by the charcoal suspension. In wild-type mice, the intestinal transit rate in GIP-administered mice was significantly less than that in saline-administered control (45 ± 8% vs. 68 ± 4%, $P < 0.01$; Fig. 3A). On the other hand, in GIPR$^{-/-}$ mice, the intestinal transit rate was similar to that in saline-administered control and GIP-administered mice (65 ± 3% vs. 63 ± 4%; Fig. 3B).

3.4. Perfusion and intestinal transit in GLP-1 receptor-deficient mice

To determine whether GIP affects intestinal glucose absorption through GLP-1 signaling, inhibition of glucose absorption by GIP was measured in GLP-1R$^{-/-}$ mice. Inhibition of glucose absorption in GLP-1R$^{-/-}$ mice was 44 ± 100 nmol/cm/15 min in saline-administered control mice and 426 ± 104 nmol/cm/15 min in GIP-administered mice (50 nmol/kg body weight, $P < 0.05$, Fig. 3C). Thus, GIP significantly inhibited glucose absorption in GLP-1R$^{-/-}$ mice.

The intestinal transit rate was also evaluated in GLP-1R$^{-/-}$ mice, and was 59 ± 13% in saline-administered control and 42 ± 7% in GIP-administered mice, respectively. Thus, GIP significantly inhibited the intestinal transit rate in GLP-1R$^{-/-}$ mice ($P < 0.01$, Fig. 3D). Consequently, the genetic disruption of GLP-1 receptor did not affect GIP action on intestinal glucose absorption and intestinal transit.

3.5. Involvement of SST in the action of GIP

To determine whether the inhibitory effect of GIP on intestinal transit is due to release of SST, a somatostatin receptor antagonist, CSS (1 μg/kg body weight), was intraperitoneally administered 10 min prior to GIP administration in wild-type mice (Fig. 4A). In the presence of CSS, the intestinal transit rate in GIP-administered wild-type mice was significantly higher than that in the absence of CSS (60 ± 3% vs. 45 ± 8%; $P < 0.01$). Accordingly, CSS reduced the inhibitory effect of GIP on intestinal transit. Moreover, intraperitoneally-administered SST itself significantly inhibited the intestinal transit rate in wild-type mice compared to control (SST: 37 ± 5% vs. control: 68 ± 4%, $P \leqslant 0.01$).

In a perfusion experiment, to confirm that the inhibitory effect of GIP on intestinal glucose absorption is attributable to release of SST, CSS (1 μg/kg body weight) was intraperitoneally administered 10 min prior to GIP administration in wild-type mice (Fig. 4B). In

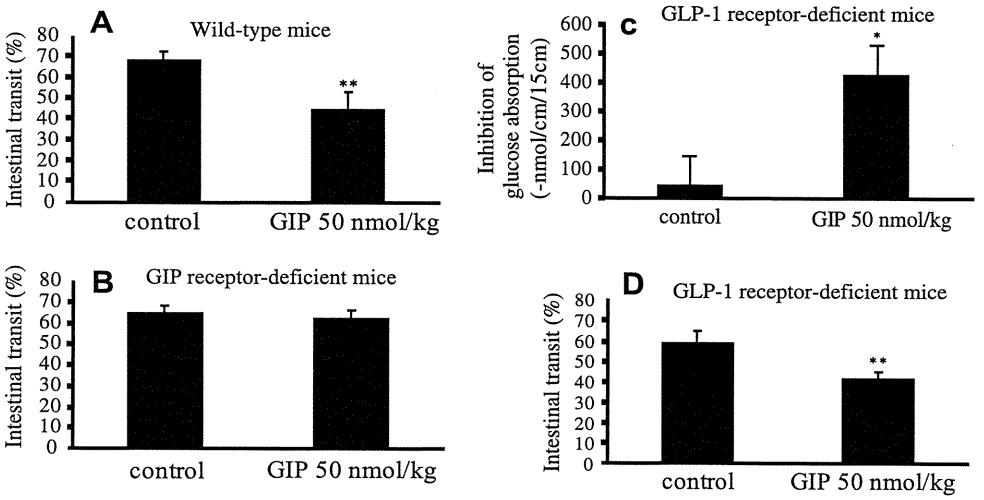

Fig. 3. Intestinal transit after oral administration of non-absorbed marker (10% charcoal suspension in 5% gum Arabic) in wild-type (A) and GIPR$^{-/-}$ (B) mice. Twenty minutes after administration of non-absorbed marker by gavage, the animals were killed and the entire gastrointestinal transit tract was removed. GIP (50 nmol/kg body weight) or saline was administered intraperitoneally 15 min prior to the administration of non-absorbed marker. Data are shown as means with SEM ($n = 6$ for each group). Statistical significance was determined using Student's t-test. **$P < 0.01$ compared with control. (C) Inhibition of glucose absorption in GLP-1R$^{-/-}$ mice with or without intraperitoneal GIP administration as indicated in the legends of Fig 1. (D) Intestinal transit after oral administration of non-absorbed marker in GLP-1R$^{-/-}$ mice with or without intraperitoneal GIP administration as indicated in the legends of Fig 3A. Data are shown as means with SEM ($n = 6$ for each group). Statistical significance was determined using Student's t-test. *$P < 0.05$ compared with control.

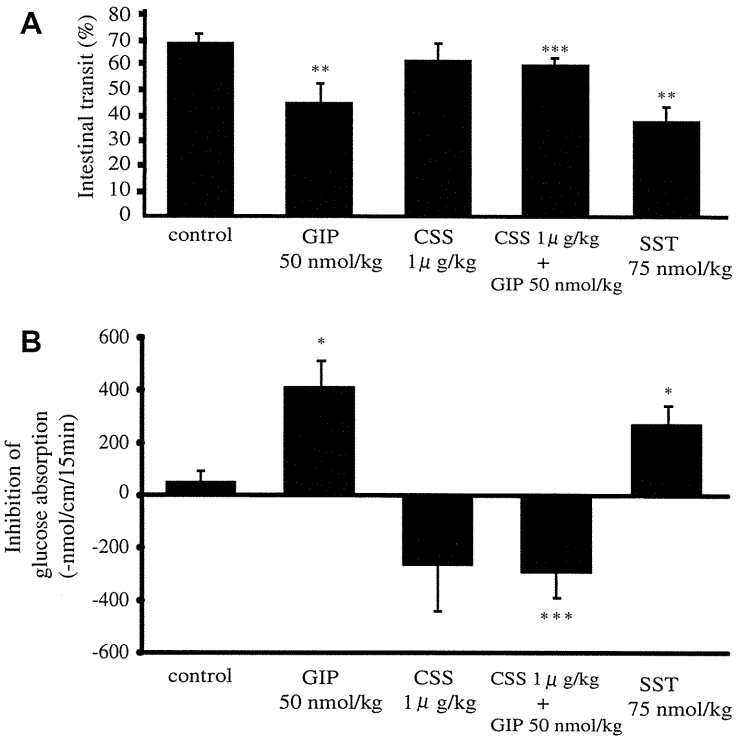

Fig. 4. (A) Intestinal transit after oral administration of non-absorbed marker in wild-type mice with or without pretreatment of CSS. The rate of transit was determined as indicated in the legend of Fig 3A. GIP or SST or saline was administered intraperitoneally 15 min prior to the administration of non-absorbed marker. CSS or saline was intraperitoneally administered 10 min prior to GIP administration. Data are shown as means with SEM ($n = 6$ for each group). Statistical significance was determined using Student's t-test. $^{**}P < 0.01$ compared with control. $^{***}P < 0.01$ compared with GIP alone administered mice. (B) Inhibition of glucose absorption by GIP in wild-type mice with or without pretreatment of CSS, and inhibition of glucose absorption by SST. CSS or saline was intraperitoneally administered 10 min prior to GIP administration. Data are shown as means with SEM ($n = 6$ for each group). Statistical significance was determined using Student's t-test. $^{*}P < 0.05$ compared with control. $^{***}P < 0.01$ compared with GIP alone administered mice.

the presence of CSS, the inhibition of glucose absorption in GIP-administered wild-type mice was significantly lower than that in the absence of CSS (410 ± 96 nmol/cm/15 min vs. −290 ± 99 nmol/cm/15 min; $P < 0.01$). Accordingly, CSS reduced the inhibitory effect of GIP on intestinal glucose absorption. Furthermore, inhibition of glucose absorption in wild-type mice was 49 ± 44 nmol/cm/15 min in saline-administered control mice and 278 ± 63 nmol/cm/15 min in SST-administered mice (75 nmol/kg body weight, $P < 0.05$).

In an experiment of glucose uptake in everted jejunal ring, 100 nM SST did not alter glucose uptake compared to control (control: 4.2 ± 0.9 μmol/g weight; SST: 4.2 ± 0.4, $n = 8$; P = NS).

3.6. Measurement of plasma GIP and SST levels

The plasma levels of total GIP and SST in mice were significantly enhanced 20 min after the intraperitoneal GIP-administration at a dosage of 50 nmol/kg body weight compared to the respective basal levels (GIP: 58 ± 5 pg/ml vs. 3400 ± 257 pg/ml, $n = 8$; $P < 0.01$; SST: 9.9 ± 0.5 ng/ml vs.11.9 ± 0.3 ng/ml, $n = 8$; $P < 0.05$).

4. Discussion

We investigated the inhibitory effect of exogenous GIP on glucose absorption in small intestine. GIP has been known as an important insulinotropic hormone released from duodenal K cells. However, there have been few reports on the effects of GIP on intestinal glucose absorption. In this study, GIP was found to inhibit glucose absorption in a concentration-dependent manner by the perfusion method.

Glucose absorption includes two steps in enterocytes, permeation through brush-border membrane and subsequently through basolateral membrane. Glucose and galactose cross the brush-border membrane by means of SGLT-1, which is a rate-limiting step of glucose absorption [10]. Recent *in vitro* study by Singh et al. found that exogenous GIP stimulates SGLT-dependent glucose absorption by using an Ussing chamber experiment [11]. In the experiment, intestine was fixed between two chambers, and short-circuit-current representing SGLT activity was measured. However, in our experiments using everted jejunal rings, which is another method to measure SGLT-dependent glucose absorption *in vitro*, the lack of effect of exogenous GIP on SGLT-dependent glucose uptake was shown, and genetic disruption of the GIP receptor was found not to affect SGLT-dependent glucose absorption. The reason why our results and theirs are different is unknown, but may be attributable to difference in method.

It is generally accepted that there is a positive relationship between intestinal motility and absorption [4,5]. It has been shown that increased intestinal motility, besides enhancing the functional surface area, facilitates diffusion of glucose to the transporters of the brush-border membrane by altering the unstirred water layer [12,13]. We investigated the effect of GIP on motility of small intestine by evaluating intestinal transit. In this study, GIP was found to inhibit intestinal transit compared to control in wild-type but not in $GIPR^{-/-}$ mice. Thus, the inhibitory effect of GIP on glucose absorption may be attributable, in part, to inhibition of intestinal motility.

GLP-1, another incretin hormone, is secreted from L cells found predominantly in ileal mucosa, and is known to be part of the "ileal brake" that acts as an inhibitor of upper gastrointestinal motility

[14]. In this study, GIP was found to inhibit intestinal transit in GLP-1R$^{-/-}$ mice as well as in wild-type mice, indicating that the inhibitory action of GIP on gastrointestinal transit is not mediated by GLP-1. Furthermore, glucose absorption was found to be inhibited significantly by GIP in GLP-1R$^{-/-}$ mice as well as in wild-type mice, suggesting that the primary mechanism of the inhibition of intestinal glucose absorption by GIP most likely does not involve the GLP-1-mediated pathway.

Recently, Miki et al. reported that GLP-1 inhibited gut motility while GIP did not [15]. In this study, however, GIP was found to inhibit intestinal transit. The inconsistency could be due to their use of a non-absorbed marker containing a high concentration (as much as 50%) of glucose to evaluate gut motility, whereas we used a non-absorbed marker without glucose. Intraduodenal infusion of hyperosmolar solution was reported to increase duodenal motility, which is mediated by activation of osmoreceptors in duodenum [16]. In our preliminary experiment on small intestinal transit using 10% charcoal suspension in 5% gum Arabic with 50% glucose, the intestinal transit rate was significantly greater than that when using glucose-free solution (88 ± 8% vs. 68 ± 4%, $P < 0.05$, unpublished data). Therefore, intestinal transit might be enhanced by the high concentration of glucose itself in the suspension, which could conceal a GIP-evoked inhibitory effect on intestinal transit. However, limitations of this study must be considered. While GIP was found to inhibit intestinal transit under the conditions of this study, the effect of GIP on intestinal transit may differ among the constituents of the food or nutrient. Further investigations are required.

Regarding the GIP dosage applied in the *in vivo* experiments, low GIP dosage has been used when applied by the route of continuous intravenous administration; GIP (0.25 nmol/kg body weight) was reported to stimulate insulin secretion by intravenous administration in rat [17] and (GIP 4 pmol/kg body weight/min) in human [18]. However, high GIP dosage has been used when applied by the other routes of administration than intravenous administration. Indeed, one group has reported that subcutaneous pre-administration of 100 μg GIP (approximately 800 nmol/kg body weight) lowered glucose excursion in oral glucose tolerance test in mice [15] and another group has reported that intraperitoneal administration of [D-Ala^2]GIP (48 nmol/kg body weight/day), a DPP4-resistant analogue, lowered glucose excursion in intraperitoneal glucose tolerance test in mice [19]. In this study, we applied GIP intraperitoneally at a dosage of 50 nmol/kg body weight to demonstrate the pharmacological effects of GIP on intestinal transit and glucose absorption, which dosage is comparable to those used in the latter reports.

Regarding the mechanism of inhibition of intestinal transit by GIP, SST secretion has been reported to be stimulated by GIP [20–22] and to prolong intestinal transit [23,24]. The SST receptor has five isoforms (sst1-5) and all five receptors have been shown to be expressed in gastrointestinal tract, with high levels of sst2 receptor in intestine [25]. The sst2 receptors in intestine have been shown not to be expressed on enterocytes or muscle cells, but on myenteric and submucosal plexuses and on neuroendocrine cells in epithelium [26] and also on interstitial cells of Cajal in deep muscular plexus [27]. Thus, the mechanisms by which exogenous GIP inhibits intestinal motility through two SST-mediated pathways may be as follows. In the first, exogenous GIP binds to the GIP receptors on the cell surface membrane in SST-containing enteric neurons and/or in mucosal endocrine cells of D cells in gastrointestinal tract and/or in pancreatic islets, resulting in the release of SST. Subsequently, the released SST acts as a neurotransmitter and binds to sst2 receptors expressed on other neurons in myenteric plexus, parts of which nerve fibers are distributed to muscular cells, permitting inhibition of intestinal motility. In this pathway, the local SST concentration in interneural synaptic space may be increased prominently. In an alternate pathway, SST secreted from D cells flows into systemic circulation through submucosal vessels to reach the neurons in myenteric plexus. Indeed, in this study, intraperitoneally-administered GIP induced a small but significant increase in plasma SST levels, suggesting involvement of the latter pathway.

In our experiment of intestinal perfusion, GIP was found to inhibit intestinal glucose absorption primarily by reducing intestinal motility. On the other hand, the tissue of everted intestinal ring is set inside-out and distended far from the physiological condition, and thus incapable of reflecting general intestinal motility. Thus, the lack of GIP action on glucose uptake in the tissues of everted intestinal ring in this study may be expected.

Several studies have found that the inhibitory effect of SST on intestinal glucose absorption may be attributable to either the effect of SST on the splanchnic hemodynamics [28] or a direct effect of SST on enterocytes [29]. However, consistent with this study, another study has found that SST delays intestinal glucose absorption by its inhibitory effect on intestinal motility [24]. SST exerts its inhibitory effect on intestinal glucose absorption by several mechanisms; our results indicate that the inhibitory effect of SST is mediated, at least in part, by alteration of intestinal motility.

In this study, the somatostatin receptor antagonist CSS was found to reduce the inhibitory effect of GIP on intestinal transit, suggesting that GIP stimulates SST release. In addition, we show that SST itself inhibits intestinal transit and glucose absorption in perfused intestine. Consistently, a recent study has reported that SST inhibits intestinal glucose absorption [29]. Considered together with previous reports, we conclude that exogenous GIP inhibits intestinal transit and glucose absorption indirectly through a somatostatin-mediated pathway.

One of the physiological roles of GIP is known to be facilitation of nutrient uptake into adipose tissue and bone. In this study, exogenous GIP was found to inhibit intestinal glucose absorption by reducing intestinal motility. Since this observation was obtained by the action of a supraphysiological level of plasma GIP, it is unclear whether or not the action is associated with already known physiological actions of GIP. In the point of delay of intestinal carbohydrate absorption, however, the biological action of GIP found in this study appears to be similar to that of medical medicine α-glucosidase inhibitor, which does not influence the regulation of energy accumulation in adipose tissue or bone.

Acknowledgments

This study was supported by Scientific Research Grants and a Grant for Leading Project for Biosimulation from the Ministry of Education, Culture, Sports, Science, and Technology of Japan, a grant from CREST of Japan Science and Technology Cooperation, and a grant from the Ministry of Health, Labor, and Welfare, Japan, and also by Kyoto University Global COE Program "Center for Frontier Medicine". The authors are grateful to Dr. Daniel J. Drucker for kindly providing GLP-1R$^{-/-}$ mice.

References

[1] Y. Seino, M. Fukushima, D. Yabe, GIP and GLP-1, the two incretin hormones: similarities and differences, J. Diabetes Invest. 1 (2010) 8–23.
[2] K. Miyawaki, Y. Yamada, H. Yano H, et al., Glucose intolerance caused by a defect in the entero-insular axis: a study in gastric inhibitory polypeptide receptor knockout mice, Proc. Natl. Acad. Sci. USA 96 (1999) 14843–14847.
[3] T.B. Usdin, E. Mezey, D.C. Button, et al., Gastric inhibitory polypeptide receptor, a member of the secretin-vasoactive intestinal peptide receptor family, is widely distributed in peripheral organs and the brain, Endocrinology 133 (1993) 2861–2870.
[4] M. Sababi, U.H. Bengtsson, Enhanced intestinal motility influences absorption in anaesthetized rat, Acta Physiol. Scand. 172 (2001) 115–122.
[5] A.J. Smout, Small intestinal motility, Curr. Opin. Gastroenterol. 20 (2004) 77–81.

[6] L.A. Scrocchi, T.J. Brown, N. MaClusky, et al., Glucose intolerance but normal satiety in mice with a null mutation in the glucagon-like peptide 1 receptor gene, Nat. Med. 2 (1996) 1254–1258.
[7] R. Athman, A. Tsocas, O. Presset, et al., In vivo absorption of water and electrolytes in mouse intestin, Application to villin$^{-/-}$ mice, Am. J. Physiol. Gastrointest. Liver Physiol. 282 (2002) G634–639.
[8] K. Tsukiyama, Y. Yamada, K. Miyawaki, et al., Gastric inhibitory polypeptide is the major insulinotropic factor in K(ATP) null mice, Eur. J. Endocrinol. 151 (2004) 407–412.
[9] K. Yamada, M. Hosokawa, S. Fujimoto, et al., The spontaneously diabetic Torii rat with gastroenteropathy, Diabetes Res. Clin. Pract. 75 (2007) 127–134.
[10] M.A. Hediger, M.J. Coady, T.S. Ikeda, et al., Expression cloning and cDNA sequencing of the Na^+/glucose co-transporter, Nature 330 (1987) 379–381.
[11] S.K. Singh, A.C. Bartoo, S. Krishnan, et al., Glucose-dependent insulinotropic polypeptide (GIP) stimulates transepithelial glucose transport, Obesity 16 (2008) 2412–2416.
[12] F.A. Wilson, J.M. Dietschy, The intestinal unstirred layer: its surface area and effect on active transport kinetics, Biochim. Biophys. Acta 363 (1974) 112–126.
[13] D.V. Rayner, The relationships between glucose absorption and insulin secretion and the migrating myoelectric complex in the pig, Exp. Physiol. 76 (1991) 67–76.
[14] A. Wettergren, B. Schjoldager, P.E. Mortensen, et al., Truncated GLP-1 (proglucagon 78–107-amido) inhibits gastric and pancreatic functions in man, Dig. Dis. Sci. 38 (1993) 665–673.
[15] T. Miki, K. Minami, H. Shinozaki, et al., Distinct effects of glucose-dependent insulinotropic polypeptide and glucagon-like peptide-1 on insulin secretion and gut motility, Diabetes 54 (2005) 1956–1963.
[16] H.C. Lin, J.D. Elashoff, G.M. Kwok, et al., Stimulation of duodenal motility by hyperosmolar mannitol depends on local osmoreceptor control, Am. J. Physiol. 266 (1994) G940–943.
[17] E.L. Mazzaferri, L. Ciofalo, L.A. Waters, et al., Effects of gastric inhibitory polypeptide on leucine- and arginine-stimulated insulin release, Am. J. Physiol. 245 (1983) E114–E120.
[18] T. Vilsbøll, T. Krarup, S. Madsbad, et al., Defective amplification of the late phase insulin response to glucose by GIP in obese Type II diabetic patients, Diabetologia 45 (2002) 1111–1119.
[19] B.J. Lamont, D.J. Drucker, Differential antidiabetic efficacy of incretin agonists versus DPP-4 inhibition in high fat fed mice, Diabetes 57 (2008) 190–198.
[20] J. Szecówka, V. Grill, E. Sandberg, et al., Effect of GIP on the secretion of insulin and somatostatin and the accumulation of cyclic AMP in vitro in the rat, Acta Endocrinol. (Copenh) 99 (1982) 416–421.
[21] L. Hansen, J.J. Holst, The effects of duodenal peptides on glucagon-like peptide-1 secretion from the ileum. A duodeno–ileal loop?, Regul Pept. 110 (2002) 39–45.
[22] J.J. Holst, S.L. Jensen, S. Knuhtsen, et al., Effect of vagus, gastric inhibitory polypeptide, and HCl on gastrin and somatostatin release from perfused pig antrum, Am. J. Physiol. 244 (1983) G515–522.
[23] G.J. Krejs, Effect of somatostatin and absorption and atropine infusion on intestinal transit tine and fructose absorption in the perfused human jejunum, Diabetes 33 (1984) 548–551.
[24] C. Johansson, O. Wisén, S. Efendić, et al., Effects of somatostatin on gastrointestinal propagation and absorption of oral glucose in man, Digestion 22 (1981) 126–137.
[25] K. Krempels, B. Hunyady, A.M. O'Carroll, et al., Distribution of somatostatin receptor messenger RNAs in the rat gastrointestinal tract, Gastroenterology 112 (1997) 1948–1960.
[26] M. Gugger, B. Waser, A. Kappeler, et al., Cellular detection of sst2A receptors in human gastrointestinal tissue, Gut 53 (2004) 1431–1436.
[27] C. Sternini, H. Wong, S.V. Wu, et al., Somatostatin 2A receptor is expressed by enteric neurons, and by interstitial cells of Cajal and enterochromaffin-like cells of the gastrointestinal tract, J. Comp. Neurol. 386 (1997) 396–408.
[28] J. Wahren, Influence of somatostatin on carbohydrate disposal and absorption in diabetes mellitus, Lancet 2 (1976) 1213–1216.
[29] F. Féry, L. Tappy, P. Schneiter, et al., Effect of somatostatin on duodenal glucose absorption in man, J. Clin. Endocrinol. Metab. 90 (2005) 4163–4169.

ORIGINAL ARTICLE

Exendin-4 Suppresses Src Activation and Reactive Oxygen Species Production in Diabetic Goto-Kakizaki Rat Islets in an Epac-Dependent Manner

Eri Mukai,[1,2] Shimpei Fujimoto,[1] Hiroki Sato,[1] Chitose Oneyama,[3] Rieko Kominato,[1] Yuichi Sato,[1] Mayumi Sasaki,[1] Yuichi Nishi,[1] Masato Okada,[3] and Nobuya Inagaki[1,4]

OBJECTIVE—Reactive oxygen species (ROS) is one of most important factors in impaired metabolism secretion coupling in pancreatic β-cells. We recently reported that elevated ROS production and impaired ATP production at high glucose in diabetic Goto-Kakizaki (GK) rat islets are effectively ameliorated by Src inhibition, suggesting that Src activity is upregulated. In the present study, we investigated whether the glucagon-like peptide-1 signal regulates Src activity and ameliorates endogenous ROS production and ATP production in GK islets using exendin-4.

RESEARCH DESIGN AND METHODS—Isolated islets from GK and control Wistar rats were used for immunoblotting analyses and measurements of ROS production and ATP content. Src activity was examined by immunoprecipitation of islet lysates followed by immunoblotting. ROS production was measured with a fluorescent probe using dispersed islet cells.

RESULTS—Exendin-4 significantly decreased phosphorylation of Src Tyr416, which indicates Src activation, in GK islets under 16.7 mmol/l glucose exposure. Glucose-induced ROS production (16.7 mmol/l) in GK islet cells was significantly decreased by coexposure of exendin-4 as well as PP2, a Src inhibitor. The Src kinase–negative mutant expression in GK islets significantly decreased ROS production induced by high glucose. Exendin-4, as well as PP2, significantly increased impaired ATP elevation by high glucose in GK islets. The decrease in ROS production by exendin-4 was not affected by H-89, a PKA inhibitor, and an Epac-specific cAMP analog (8CPT-2Me-cAMP) significantly decreased Src Tyr416 phosphorylation and ROS production.

CONCLUSIONS—Exendin-4 decreases endogenous ROS production and increases ATP production in diabetic GK rat islets through suppression of Src activation, dependently on Epac. ***Diabetes* 60:218–226, 2011**

From the [1]Department of Diabetes and Clinical Nutrition, Graduate School of Medicine, Kyoto, University, Kyoto, Japan; the [2]Japan Association for the Advancement of Medical Equipment, Tokyo, Japan, the [3]Department of Oncogene Research, Research Institute for Microbial Diseases, Osaka University, Osaka, Japan; and the [4]Core Research for Evolutional Science and Technology of Japan Science and Technology Cooperation, Kyoto, Japan.

Corresponding author: Shimpei Fujimoto, fujimoto@metab.kuhp.kyoto-u.ac.jp.

Received 6 January 2010 and accepted 12 October 2010. Published ahead of print at http://diabetes.diabetesjournals.org on 26 October 2010. DOI: 10.2337/db10-0021.

In pancreatic β-cells, glucose metabolism regulates exocytosis of insulin granules through metabolism secretion coupling, in which glucose-induced ATP production in mitochondria plays an essential role (1). Impairment of mitochondrial ATP production causes reduced glucose-induced insulin secretion.

Reactive oxygen species (ROS) is one of the most important factors that impair metabolism secretion coupling in β-cells. Exposure to exogenous hydrogen peroxide (H_2O_2), the most abundant ROS, reduces glucose-induced insulin secretion by impairing mitochondrial metabolism in β-cells (2,3). However, little is known of the role of endogenous ROS in impaired glucose-induced insulin secretion from β-cells. Some studies (4,5) have shown that endogenous ROS is produced in mitochondria by exposure to high glucose. In Zucker diabetic fatty rats, the superoxide content of islets at basal glucose levels is higher than that in Zucker lean control rats (4). Furthermore, we recently reported that high glucose–induced ROS production in islet cells is elevated in diabetic Goto-Kakizaki (GK) rats compared with control Wistar rats (6). Thus, endogenous ROS production is elevated in β-cells under diabetic pathophysiological conditions.

Although the mechanism of endogenous ROS production in β-cells in the diabetic state remains largely unknown, we have reported that Src (c-Src) plays an important role in the signal transduction that produces ROS (6). Src is a nonreceptor tyrosine kinase that is associated with the cell membrane and plays important roles in various signal transductions, and its activity is regulated by intramolecular interactions that depend on tyrosine phosphorylation (7,8). Phosphorylation of Tyr527 (Tyr529 in humans), which is located near the C terminus of Src, is brought about by COOH terminal Src kinase (Csk), a negative regulator of Src (9), and holds the kinase in the inactive form. Dephosphorylation of Tyr527 followed by disruption of the intramolecular interaction allows phosphorylation of Tyr416 (Tyr418 in humans) at the kinase domain, resulting in Src activation. In our previous report (6), PP2, a selective Src inhibitor, decreased high-glucose–induced ROS production in GK islet cells, in contrast to the lack of any effect of the agent in Wistar islet cells, suggesting that Src may be activated in the diabetic condition and cause elevation of ROS production in the presence of high glucose.

Glucagon-like peptide (GLP)-1 is one of the incretin peptides released from the intestine in response to nutrient ingestion that augments glucose-induced insulin secretion from β-cells (10,11). GLP-1 binding to the GLP-1 receptor, a member of the G protein–coupled receptor

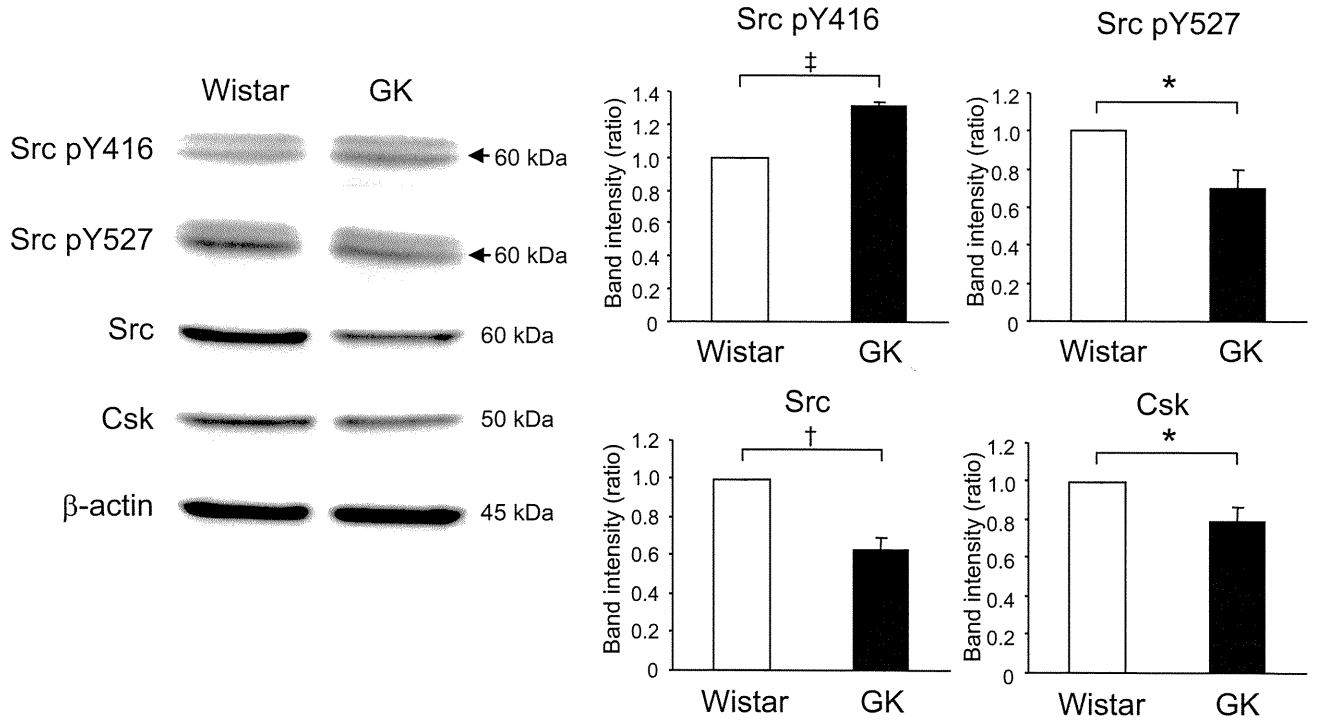

FIG. 1. Comparison of expression of Src between fresh Wistar and GK islets. Fresh islets were lysated and subjected to immunoblot analyses. Blots (50 μg of protein) were probed with anti–phospho-Src (Tyr^{416}), anti–phospho-Src (Tyr^{527}), anti-Src, or anti-Csk. The same blots were stripped and reprobed with anti–β-actin, respectively. Intensities of the bands were quantified with densitometric imager. The bar graphs are expressed relative to Wistar islet value corrected by β-actin level (means ± SE). *$P < 0.05$; †$P < 0.01$; ‡$P < 0.001$. Representative blot panels of three to five independent experiments are shown.

(GPCR) superfamily, induces activation of adenylyl cyclase and elevation of intracellular cAMP levels, which elicits protein kinase A (PKA)-dependent signal transduction. Recently, Epac (also known as cAMP-GEF [guanine nucleotide exchange factor]) has been shown to be a novel cAMP sensor in the PKA-independent pathway (12,13). In β-cells, one member of the Epac family, Epac2, has an important role in insulin secretion, especially in regulation of exocytosis of insulin granules (14,15). Previous studies have shown that GLP-1 also has beneficial long-term effects on diabetic β-cells, including induction of β-cell proliferation (16,17), enhanced resistance to apoptosis (17,18), and amelioration of endoplasmic reticulum stress (19). Furthermore, increased ROS in diabetic *db/db* mouse islets is decreased by treatment with an inhibitor of dipeptidyl peptidase IV that delays the degradation of GLP-1 (20).

In the present study, we investigated whether the GLP-1 signal directly ameliorates endogenous ROS production in diabetic GK islets using exendin-4, a GLP-1 receptor agonist. In particular, we focused on clarifying regulation of Src activity by GLP-1 signaling. We describe here both a novel effect and a mechanism of GLP-1 signaling that acutely decreases ROS production by high glucose through suppression of Src activation PKA independently and Epac dependently.

RESEARCH DESIGN AND METHODS

Male Wistar and GK rats were obtained from Shimizu (Kyoto, Japan). All experiments were carried out with rats that were aged ~7–8 weeks. Nonfasting blood glucose levels were ~160–240 mg/dl in the GK rats and ~70–120 mg/dl in the Wistar rats used in the experiments. The animals were maintained and used in accordance with the guidelines of the animal care committee of Kyoto University.

Islet preparation. Pancreatic islets were isolated from Wistar and GK rats by the collagenase digestion technique (6). Isolated islets were washed with Krebs Ringer bicarbonate buffer (KRBB) (in mmol/l: 129.4 NaCl, 5.2 KCl, 2.7 $CaCl_2$, 1.3 KH_2PO_4, 1.3 $MgSO_4$, and 24.8 $NaHCO_3$ [equilibrated with 5% CO_2/95% O_2, pH 7.4]) containing 2.8 mmol/l glucose and cultured for ~20 h in RPMI-1640 medium containing 5.5 mmol/l glucose and 10% FCS. Cultured islets were preincubated for 30 min at 37°C in KRBB supplemented with 0.2% BSA and 10 mmol/l HEPES (KRBB medium) containing 2.8 mmol/l glucose and incubated for the indicated times at 37°C in KRBB medium containing 16.7 mmol/l glucose with or without test materials.

Retroviral-mediated gene transfer. Production of retroviral vectors with pCX4 was performed as previously described (21). Src kinase–negative mutant (K295M) was subcloned into pCX4pur (22). Gene transfer experiments of islets were carried out by an in vivo gene transduction method (23). Briefly, after rats were anesthetized and subjected to laparotomy, the hepatic artery with the portal vein and the splenic artery were ligated. The upper side of the celiac artery that branches from the abdominal aorta was clamped, and 100 μl of retroviral vector suspension was injected into the lower side of the clamped point of the artery. The pancreatic islets were then isolated and cultured for 48 h before the experiment. Gene expression using green fluorescent protein–expressing vector was effective in the inside of the islets, as previously reported (23).

Immunoprecipitation and immunoblotting. Fresh or incubated islets were lysed in ice-cold lysis buffer (10 mmol/l Tris [pH 7.2], 100 mmol/l NaCl, 1 mmol/l EDTA, 1% Nonidet P-40, and 0.5% sodium deoxycholate) containing protease inhibitor cocktail (Complete; Roche, Mannheim, Germany), phosphatase inhibitor cocktail (Calbiochem, Darmstadt, Germany), and 5 mmol/l sodium pyrophosphate. For determination of Src activation, lysates were centrifuged at 560,000*g* for 10 min at 4°C, and the supernatant (~2 mg of protein content/2,500 islets) was mixed with 4 μg mouse monoclonal anti-Src antibody (clone GD11; Upstate, Billerica, MA) and 30 μl washed protein G Sepharose (GE Healthcare, Uppsala, Sweden) followed by gentle rotation for 4 h at 4°C. Immunoprecipitates or islet lysates (50 μg) were subjected to immunoblotting as previously described (23). Primary antibodies used were rabbit anti–phospho-Src (Tyr416) and anti–phospho-Src (Tyr527) from Biosource (Camarillo, CA); rabbit anti-Src, anti-Csk, anti-Epac2, extracellular signal–regulated kinase (ERK) 1/2, and mouse anti–phospho-ERK1/2 (Thr202/Tyr204) from Santa Cruz Biotechnology (Santa Cruz, CA); rabbit anti-Rap1 from Upstate; rabbit anti–phospho-Akt (Ser473) and anti-Akt from Cell

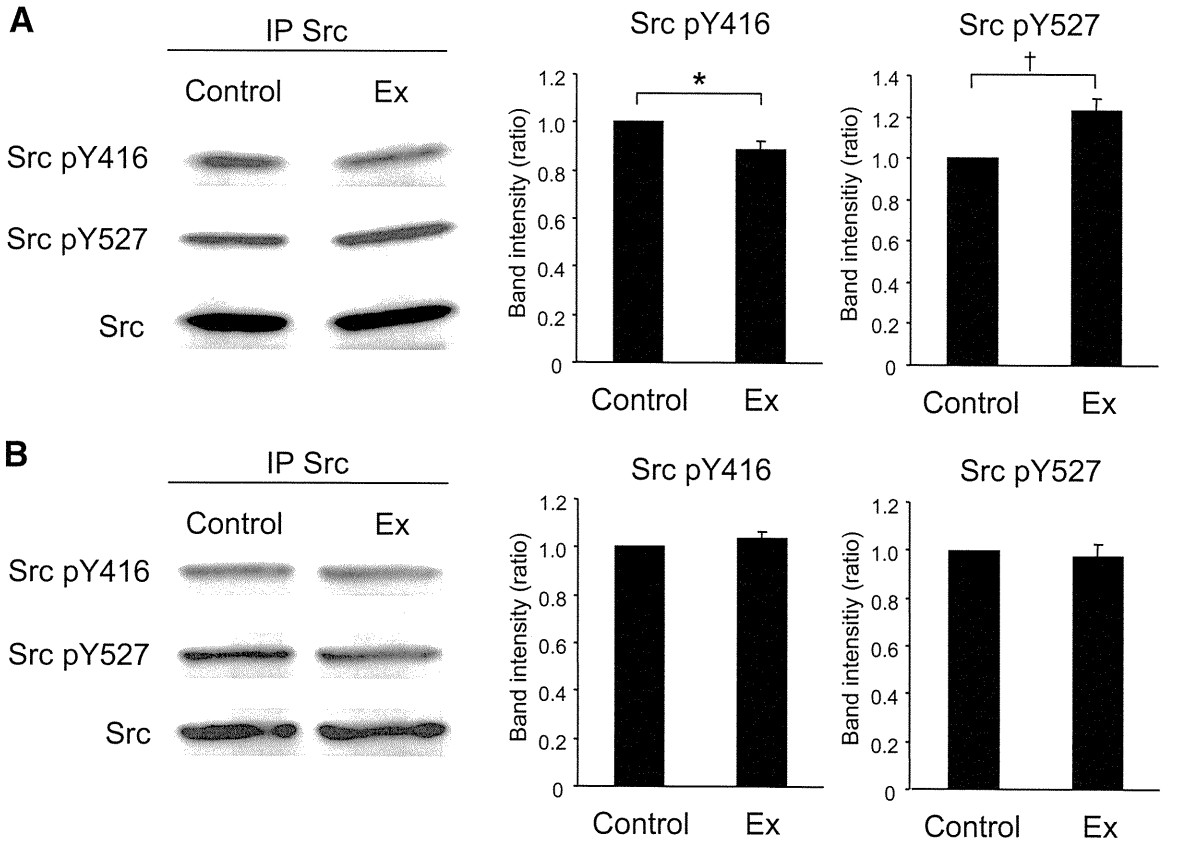

FIG. 2. Exendin-4 suppresses Src activity at high glucose in GK islets. Effects of exendin-4 on Src activity at high glucose in GK (*A*) and Wistar (*B*) islets. After preincubation in the presence of 2.8 mmol/l glucose for 30 min, islets were incubated in the presence of 16.7 mmol/l glucose with or without 100 nmol/l exendin-4 for 10 min. Islet lysates (~2 mg of protein) were immunoprecipitated with anti-Src antibody and subjected to immunoblot analyses. Blots were probed with anti–phospho-Src (Tyr^{416}), anti–phospho-Src (Tyr^{527}), or anti-Src by stripping and reprobing of the same blots. Intensities of the bands were quantified with densitometric imager. The bar graphs are expressed relative to control value corrected by Src level (means ± SE). *$P < 0.05$; †$P < 0.01$. Representative blot panels of four (*A*) or three (*B*) independent experiments are shown.

Signaling (Danvers, MA); and mouse anti–β-actin from Sigma (St. Louis, MO). Secondary antibodies used were horseradish peroxidase–conjugated anti-rabbit and mouse antibody (GE Healthcare). Band intensities were quantified with Multi Gauge software (Fujifilm, Tokyo, Japan).

Measurement of ROS production. ROS production in islet cells was measured by 2′,7′-dichlorofluorescein fluorescence (6). Briefly, cultured islets were dispersed using 0.05% trypsin/0.53 mmol/l EDTA (Invitrogen, Carlsbad, CA) and PBS. Dispersed islet cells were preincubated in KRBB medium containing 2.8 mmol/l glucose and 10 μmol/l 5-(and 6-) chloromethyl-2′,7′-dichlorodihydrofluorescein diacetate (CM-H_2DCFDA; Invitrogen) for 20 min at 37°C. After a 60-min incubation in 400 μl KRBB medium containing 16.7 mmol/l glucose with or without test materials, fluorescence was measured using a spectrofluorophotometer (RF-5300PC; Shimadzu, Kyoto, Japan), with excitation wavelength at 505 nm and emission wavelength at 540 nm. Fluorescence was corrected by subtracting parallel blanks and represented by fold increases of the value at time zero.

Measurement of ATP content. ATP content in islets was determined by luminometry as previously described (6). Briefly, after preincubation, groups of 10 islets were batch incubated for 30 min in KRBB medium containing 2.8 or 16.7 mmol/l glucose with or without test materials. Incubation was stopped immediately by addition of $HClO_4$ and sonication in ice-cold water for 10 min. They were then centrifuged, and a fraction of the supernatant was mixed with HEPES and Na_2CO_3. The ATP content in the supernatant of islet lysates was measured using ENLITEN luciferase/luciferin reagent (Promega, Madison, WI) with a luminometer (GloMax 20/20n; Promega).

Materials. Exendin-4 and forskolin were purchased from Sigma. PP2 was purchased from Tocris (Ellisville, MO). PP3, H-89, myristoylated PKA inhibitor amide14–22 (PKI), LY294002, wortmannin, PD98059, and AG1478 were purchased from Calbiochem. Dibutyryl cAMP was purchased from Daiichisankyo (Tokyo, Japan). 8-(4-chlorophenylthio)-2′-*O*-methyl-cAMP (8CPT-2Me-cAMP) was purchased from Biolog Life Science (Bremen, Germany).

Statistical analysis. Data are expressed as means ± SE. Statistical significance of difference was evaluated by the unpaired Student *t* test. $P < 0.05$ was considered significant.

RESULTS

Comparison of expression of Src between Wistar and GK islets. To examine whether the expression levels of Src in GK islets differ from those in Wistar islets, immunoblotting using fresh islets was performed. As shown in Fig. 1*A*, the level of Src pY416, which indicates activation of Src, in GK islets was significantly higher than that in Wistar islets. The levels of Src pY527, total Src, and Csk in GK islets were significantly lower than those in Wistar islets. The levels of other Src family kinases (SFKs) were similar in Wistar and GK islets, whereas the expression of Fgr was very low and that of Fyn was undetectable (supplementary Fig. 1 in the online appendix, available at http://diabetes.diabetesjournals.org/cgi/content/full/db10-0021/DC1). Results of immunoblotting using islets cultured for 20 h in the presence of 5.5 mmol/l glucose (supplementary Fig. 2) were similar to those shown in Fig. 1*A*.

Exendin-4 suppresses Src activity in GK islets. To investigate whether exendin-4 regulates Src activity, phosphorylation of Src was examined by immunoprecipitation and immunoblotting. As shown in Fig. 2*A*, Src pY416 was

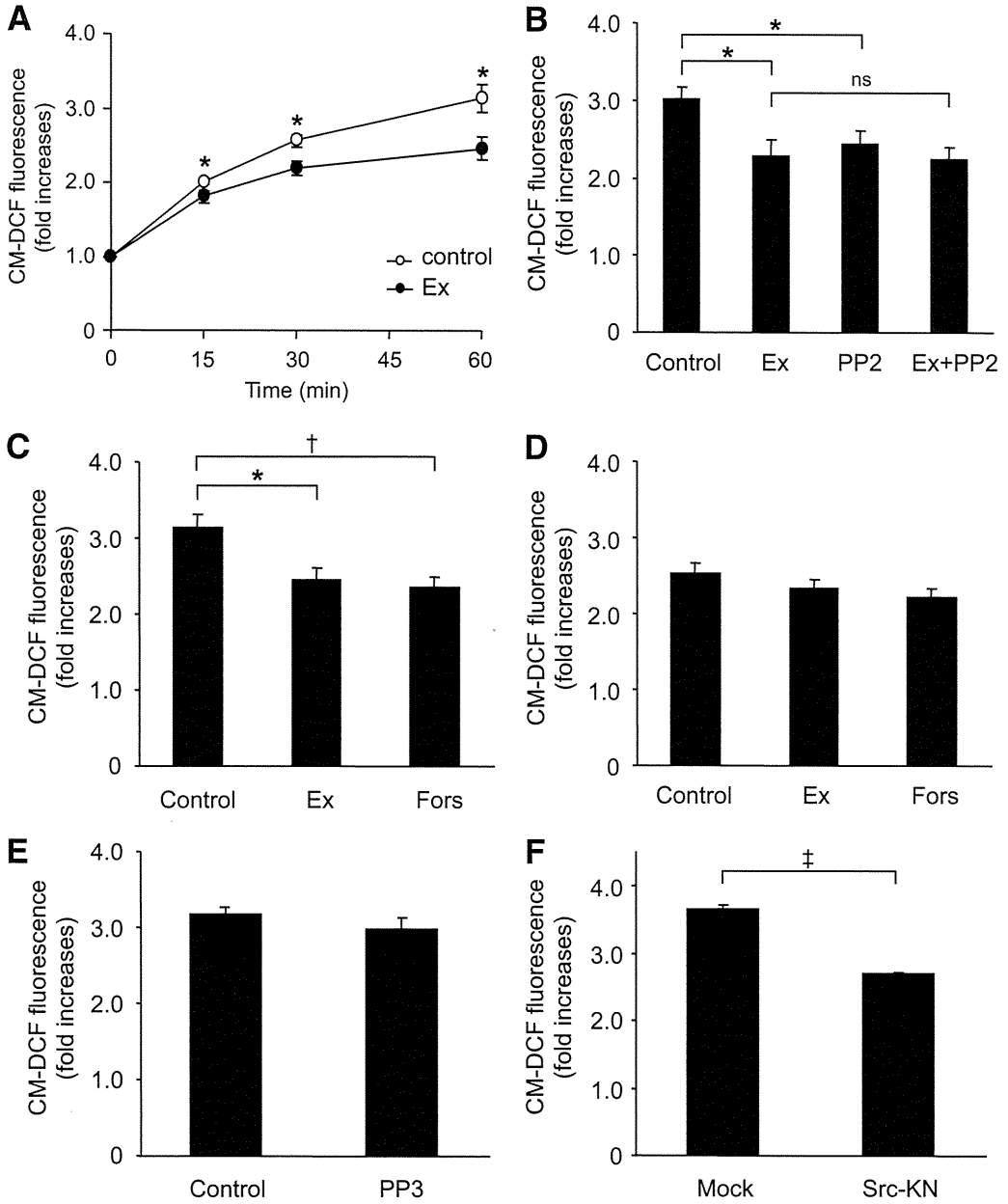

FIG. 3. Exendin-4 decreases ROS production at high glucose in GK islet cells. *A*: Time course of high-glucose–induced ROS production with or without 100 nmol/l exendin-4 in GK islet cells. After preincubation in the presence of 2.8 mmol/l glucose and 10 μmol/l CM-H_2DCFDA for 20 min, dispersed islet cells were incubated in the presence of 16.7 mmol/l glucose with (●) or without (○) 100 nmol/l exedin-4 for 60 min. Fluorescence is represented as fold increases against the value at time zero. Data are expressed as means ± SE (n = 5–7). *P < 0.05 vs. control. *B*: Effects of exendin-4 and PP2 on high-glucose–induced ROS production at 60 min in GK islet cells. Data are expressed as means ± SE (n = 4–6). *P < 0.05. *C*: Effects of exendin-4 and forskolin on high-glucose–induced ROS production at 60 min in GK islet cells. Data are expressed as means ± SE (n = 5–6). *P < 0.05; †P < 0.01. *D*: Effects of exendin-4 and forskolin on high-glucose–induced ROS production at 60 min in Wistar islet cells. Data are expressed as means ± SE (n = 3–4). *E*: Effects of PP3 on high-glucose–induced ROS production at 60 min in GK islet cells. Data are expressed as means ± SE (n = 3). *F*: Effect of Src-KN on high-glucose–induced ROS production at 60 min in GK islet cells. Retroviral (empty vector and Src-KN vector)-mediated gene transfer to islets was carried out by in vivo gene transduction method, as described in RESEARCH DESIGN AND METHODS. Data are expressed as means ± SE (n = 3). ‡P < 0.001.

significantly decreased by 100 nmol/l exendin-4 in the presence of 16.7 mmol/l glucose in GK islets. Exendin-4 also significantly increased Src pY527 in GK islets in the same condition. On the other hand, exendin-4 did not affect Src pY416 or pY527 at high glucose in Wistar islets (Fig. 2*B*). Both Src pY416 and pY527 were not altered by change in glucose concentration in GK or Wistar islets (supplementary Fig. 3).

Exendin-4 decreases ROS production in GK islet cells. We then investigated whether exendin-4 ameliorates endogenous ROS production at high glucose in GK islet cells. A total of 16.7 mmol/l glucose exposure induced ROS production in GK islet cells (Fig. 3*A*). Coexposure of exendin-4 significantly decreased ROS production in the presence of 16.7 mmol/l glucose at 15, 30, and 60 min. A total of 10 μmol/l PP2, a Src inhibitor, significantly de-

creased high-glucose–induced ROS production (Fig. 3*B*), but PP3, the inactive PP2 analog, did not affect it (Fig. 3*E*). Exendin-4 did not further decrease ROS production in the presence of PP2 (Fig. 3*B*), suggesting that the effect of exendin-4 is via the Src signal. The decrease in high-glucose–induced ROS production also was observed in the presence of 10 μmol/l forskolin, an adenylyl cyclase activator (Fig. 3*C*). High-glucose–induced ROS production in Wistar islet cells was lower than that in GK islet cells and was not changed by addition of exendin-4 or forskolin (Fig. 3*D*). To confirm that Src is actually involved in ROS production, we measured ROS production in GK islets expressing a kinase-negative form of Src (Src-KN) by retroviral vector. ROS production in Src-KN–expressing islets was significantly lower than that in control (Fig. 3*F*), demonstrating that Src regulates ROS production in GK islets.

Exendin-4 increases ATP content in GK islets. In Wistar islets, 16.7 mmol/l glucose-exposure significantly increased ATP content compared with that in the presence of 2.8 mmol/l glucose, as shown in Fig. 4*B*. Exendin-4, PP2, or exendin-4 plus PP2 did not affect the ATP content in the presence of 16.7 mmol/l glucose in Wistar islets. The ATP content in GK islets exposed to 16.7 mmol/l glucose was not increased compared with that in the presence of 2.8 mmol/l glucose (Fig. 4*A*). Exendin-4 as well as PP2 significantly increased the ATP content in the presence of 16.7 mmol/l glucose. Further increase of ATP content by combined exendin-4 and PP2 was not observed.

The effects of exendin-4 are dependent on Epac. We then investigated whether the decrease in ROS production by exendin-4 is dependent on PKA. As shown in Fig. 5*A*, decreased ROS production by exendin-4 or forskolin was not affected by 10 μmol/l H-89 or PKI, a PKA inhibitor, indicating that the effect is PKA independent. Not only dibutyryl cAMP, a general cAMP analog, but also 8CPT-2Me-cAMP, an Epac-specific cAMP analog, decreased ROS production (Fig. 5*C*). Epac possesses guanine nucleotide exchange factor activity toward Rap1, a member of the Ras superfamily of small GTPases. Epac2 and Rap1 proteins were expressed similarly in both Wistar and GK islets (Fig. 5*B*). To determine involvement of Epac in Src activation, Src phosphorylation was examined. Src pY416 was significantly decreased by 8CPT-2Me-cAMP (Fig. 5*D*).

A downstream pathway of Src is PI3K/Akt signaling. Src signalings toward downstream proteins are complex, but one of the typical pathways is phosphatidylinositol 3 kinase (PI3K)/Akt signaling (8). We therefore examined the involvement of PI3K/Akt signaling on ROS production. A total of 50 μmol/l LY294002 and 0.5 μmol/l wortmannin, both of which are PI3K inhibitors, significantly decreased ROS production in GK islets (Fig. 6*A*). Exendin-4 and PP2 both significantly decreased phosphorylation of Akt in GK islets (Fig. 6*B*) but not in Wistar islets (Fig. 6*C*). Considering these findings together, PI3K/Akt signaling that produces ROS is located downstream of Src activation. We also examined the involvement of mitogen-activated protein kinase signaling, another downstream pathway of Src. A total of 50 μmol/l PD98059, a MAPK-ERK kinase inhibitor, did not affect ROS production in GK islets (Fig. 6*D*), and neither exendin-4 nor PP2 affected phosphorylation of ERK (Fig. 6*E*). Several GPCR agonists have been shown to induce transactivation of epidermal growth factor receptor (EGFR) (24,25) by a mechanism involving Src (25–27) and frequently subsequent PI3K/Akt signaling (25,28). Therefore, involvement of EGFR transactivation on regulation of ROS production was examined. A total of 0.5 μmol/l AG1478, an EGFR kinase inhibitor, significantly decreased ROS production (Fig. 6*F*).

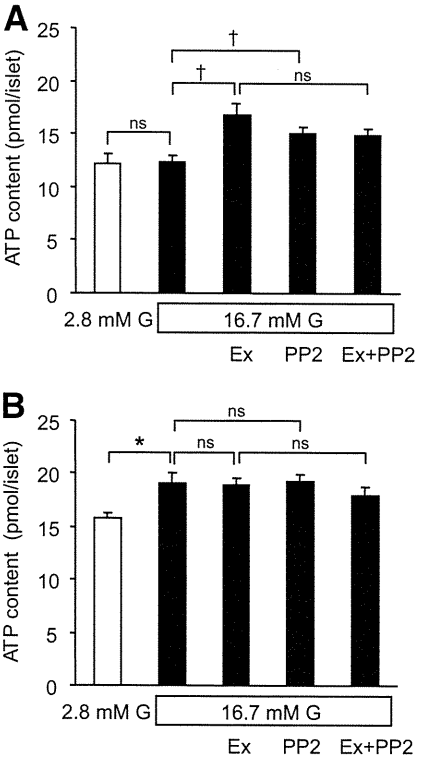

FIG. 4. Exendin-4 increases ATP content at high glucose in GK islets. Effects of exendin-4 and PP2 on ATP content in the presence of high glucose for 30 min in GK (*A*) and Wistar (*B*) islets. After preincubation in the presence of 2.8 mmol/l glucose for 30 min, islets were incubated in the presence of 2.8 or 16.7 mmol/l glucose with or without 100 nmol/l exendin-4, 10 μmol/l PP2, or both for 30 min. Data are expressed as means ± SE (n = 7–8). *P < 0.05; †P < 0.01.

DISCUSSION

We previously reported that endogenous ROS production by high glucose in diabetic GK islets is elevated compared with that in control Wistar islets and is effectively ameliorated by Src inhibition, suggesting that Src may be activated in GK islets (6). In the present study, we first investigated whether Src activity is altered in GK islets. Immunoblotting analysis revealed that the level of Src pY416, which indicates the level of Src activation, is higher in GK islets than that in Wistar islets, despite lower levels of total Src, Src pY527, and Csk. The lower level of total Src seems to be a consequence of Src activation. Targeted degradation of active forms of Src is brought about by ubiquitination (29). The protooncogene c-Cbl, recently found to be an E3 ubiquitin ligase, mediates ubiquitination of activated Src (30). These reports suggest that increased degradation of activated Src may result in a lower level of total Src in GK islets. In addition, a lower level of Csk might cause a lower activity of the kinase in GK islets. However, Src activity is not directly regulated through phosphorylation of Tyr527 by Csk (8), and a subtle decrease in Csk activity is not believed to contribute to regulation of Src activity because of the excess amount of expression of Csk. This is supported by the findings that heterozygous disruption of ubiquitously expressed Csk

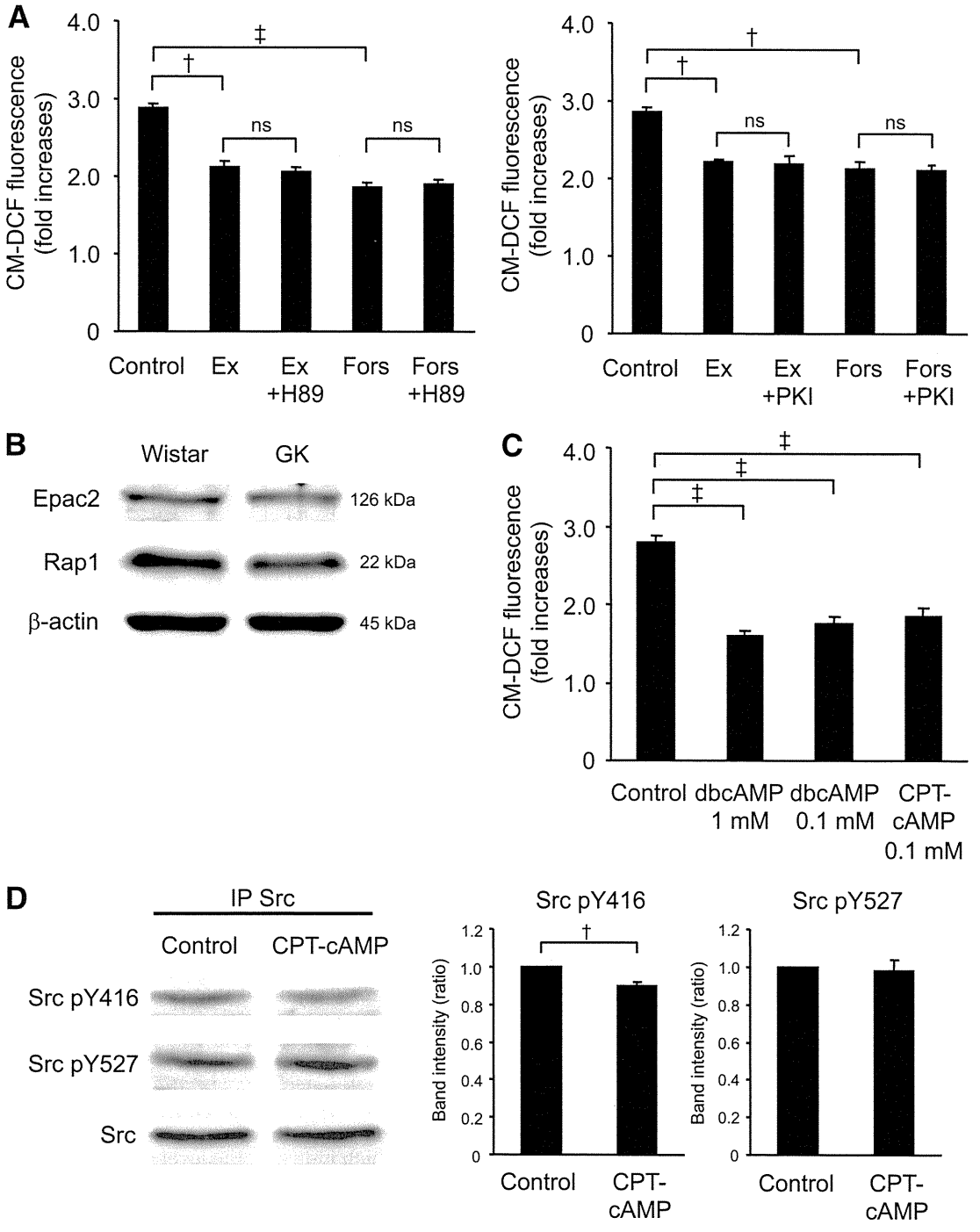

FIG. 5. The effects of exendin-4 are dependent not on PKA but on Epac. *A*: Effects of H-89 or PKI on the decrease in high-glucose–induced ROS production by exendin-4 or forskolin at 60 min in GK islet cells. After preincubation in the presence of 2.8 mmol/l glucose and 10 μmol/l CM-H_2DCFDA for 20 min, dispersed islet cells were incubated in the presence of 16.7 mmol/l glucose with or without 100 nmol/l exendin-4 or 10 μmol/l forskolin with or without 10 μmol/l H-89 or 10 μmol/l PKI for 60 min. Fluorescence is represented as fold increases against the value at time zero. Data are expressed as means ± SE (n = 3). †P < 0.01; ‡P < 0.001. *B*: Expression of Epac2 and Rap1 in Wistar and GK islets. Fresh islets were lysated and subjected to immunoblot analyses. Blots (50 μg of protein) were probed with anti-Epac2 or anti-Rap1. The same blots were stripped and reprobed with anti–β-actin, respectively. Representative blot panels of three independent experiments are shown. *C*: Effects of cAMP analogs on high-glucose–induced ROS production at 60 min in GK islet cells. Data are expressed as means ± SE (n = 3–4). ‡P < 0.001. *D*: Epac-specific cAMP analog suppresses Src activity at high glucose in GK islets. After preincubation in the presence of 2.8 mmol/l glucose for 30 min, islets were incubated in the presence of 16.7 mmol/l glucose with or without 0.1 mmol/l 8CPT-2Me-cAMP for 8 min. Islet lysates (~2 mg of protein) were immunoprecipitated with anti-Src antibody and subjected to immunoblot analyses. Blots were probed with anti–phospho-Src (Tyr^{416}), anti–phospho-Src (Tyr^{527}), or anti-Src by stripping and reprobing of the same blots. Intensities of the bands were quantified with densitometric imager. The bar graphs are expressed relative to control value corrected by Src level (means ± SE). †P < 0.01. Representative blot panels of four independent experiments are shown.

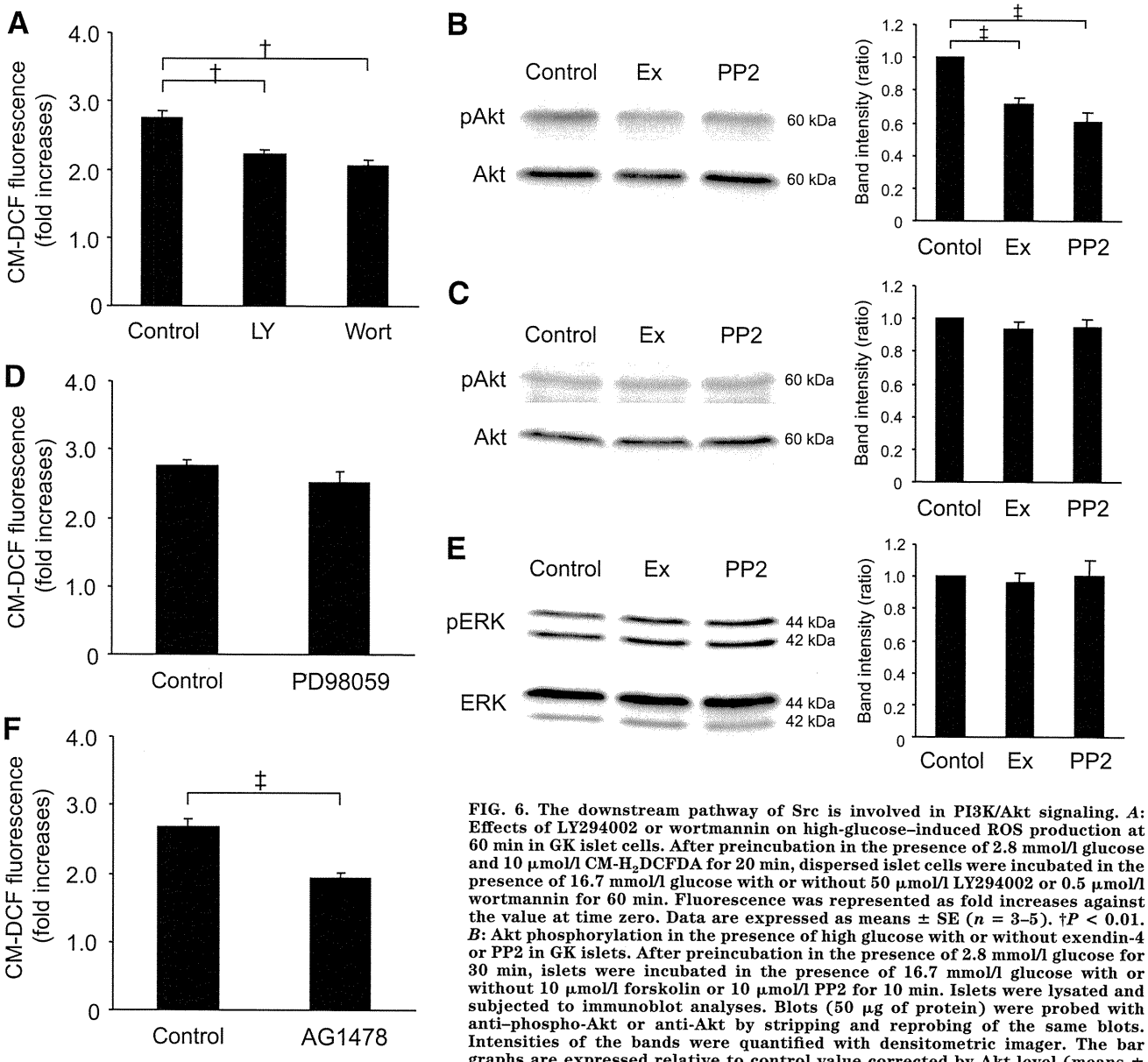

FIG. 6. The downstream pathway of Src is involved in PI3K/Akt signaling. *A*: Effects of LY294002 or wortmannin on high-glucose–induced ROS production at 60 min in GK islet cells. After preincubation in the presence of 2.8 mmol/l glucose and 10 μmol/l CM-H_2DCFDA for 20 min, dispersed islet cells were incubated in the presence of 16.7 mmol/l glucose with or without 50 μmol/l LY294002 or 0.5 μmol/l wortmannin for 60 min. Fluorescence was represented as fold increases against the value at time zero. Data are expressed as means ± SE (n = 3–5). †P < 0.01. *B*: Akt phosphorylation in the presence of high glucose with or without exendin-4 or PP2 in GK islets. After preincubation in the presence of 2.8 mmol/l glucose for 30 min, islets were incubated in the presence of 16.7 mmol/l glucose with or without 10 μmol/l forskolin or 10 μmol/l PP2 for 10 min. Islets were lysated and subjected to immunoblot analyses. Blots (50 μg of protein) were probed with anti–phospho-Akt or anti-Akt by stripping and reprobing of the same blots. Intensities of the bands were quantified with densitometric imager. The bar graphs are expressed relative to control value corrected by Akt level (means ± SE). ‡P < 0.001. Representative blot panels of five independent experiments are shown. *C*: Akt phosphorylation in the presence of high glucose with or without exendin-4 or PP2 in Wistar islets. Representative blot panels of three independent experiments are shown. *D*: Effects of PD98059 on high-glucose–induced ROS production at 60 min in GK islet cells. Data are expressed as means ± SE (n = 4). *E*: ERK phosphorylation in the presence of high glucose with or without exendin-4 or PP2 in GK islets. Blots (50 μg of protein) were probed with anti–phospho-ERK or anti-ERK by stripping and reprobing of the same blots. The bar graphs are expressed relative to control value corrected by ERK level (means ± SE). Representative blot panels of three independent experiments are shown. *F*: Effects of AG1478 on high-glucose–induced ROS production at 60 min in GK islet cells. Data are expressed as means ± SE (n = 5). ‡P < 0.001.

does not affect the phenotype in mice, contrary to neural tube defects and embryonic lethality in homozygous deficient mice (31). Moreover, the localization of Csk in the cytosol before recruitment to the membrane for Src regulation dose not differ in Wistar and GK islets (supplementary Fig. 4). Thus, the lower expression level of Csk found in our results is not likely to play a role in the Src activation in GK islets. Activation of Src as well as elevated endogenous ROS production at high glucose in GK islets was clearly suppressed by exendin-4, which did not affect Src phosphorylation or ROS production in Wistar islets. Thus, the GLP-1 signal might well suppress activation of Src and excessive ROS production under diabetic conditions in addition to other beneficial long-term effects on β-cells.

GLP-1 induces elevation of intracellular cAMP levels and subsequent activation of PKA after binding to the GLP-1 receptor. In the present study, the effect of GLP-1 signaling, which suppresses Src activation and ROS production, was found to be independent of PKA. Epac is a PKA-independent cAMP sensor; Epac2 is expressed mainly in neuroendocrine cells including pancreatic β-cells. Epac2 regulates exocytosis of insulin granules in β-cells by mobilizing intracellular Ca^{2+} and interacting granule-associated proteins (14,15). Although the relationship between Epac and Src is not well known, a recent

report (32) has shown that cAMP protects against hepatocyte apoptosis Epac dependently through Src and PI3K/Akt activation. Further evaluation of the role of cAMP in regulation of Src and PI3K/Akt signaling is required.

In the present study, we have shown that one of these Src signals, the PI3K/Akt signal, regulates ROS production. Furthermore, GLP-1 induces β-cell proliferation through PI3K signaling via Src and EGFR transactivation (33). Our finding that the EGFR kinase inhibitor decreases ROS production suggests that EGFR transactivation may be involved in the ROS-reducing effect of exendin-4 via Src. Under normal conditions, GPCR stimulation generally activates Src toward EGFR transactivation, frequently followed by PI3K activation (25). The present study reveals that Src and PI3K activities are upregulated in islets under diabetic conditions, which are suppressed by the GLP-1 signal. Many studies in oncology have shown that several growth factors including EGF and platelet-derived growth factor induce ROS through PI3K activation (34–36). Thus, EGFR transactivation/PI3K signaling should be activated under pathophysiologically disordered conditions. In the various states between normal and diabetic conditions, the ameliorative effects of the GLP-1 signal may differ (37). Further elucidation of these signals in the pathophysiology of diabetes should be helpful in future development of therapeutic strategies.

Previous studies have shown that the antioxidant capacity in β-cells is very low because of weak expression of antioxidant enzymes in pancreatic islets compared with that in various other tissues (38). The superoxide anion is converted by superoxide dismutase (SOD) into hydrogen peroxide that is eventually removed by glutathione peroxidase (Gpx). The expression level of MnSOD, which is localized in mitochondria, was significantly lower in GK islets than in Wistar islets, and that of of Gpx was similar in Wistar and GK islets (supplementaty Fig. 5*A*). However, an enzymatic assay revealed that MnSOD activity in GK islets was similar to that in Wistar islets and that it was not affected by exendin-4 or PP2 (supplementary Fig. 5*B* and *C*). These results indicate that regulation of MnSOD activity does not play a role in the suppressive effects of ROS production by exendin-4.

One of the important sites of ROS generation in β-cells is the mitochondrial electron transport chain, in which ROS generation increases according to the hyperpolarization of mitochondrial inner membrane derived from accelerated glucose metabolism (39). However, in pathophysiological conditions, NADPH oxidase may play an important role in ROS generation in β-cells. Chronic exposure to proinflammatory cytokines and abundant nutrients including glucose and palmitate augments the expression of a phagocyte-like NADPH oxidase in β-cells (40). Moreover, the expression of NADPH oxidase is increased in islets of diabetic Otsuka Long Evans Tokushima Fatty rats (41). Because Src is involved in regulation of NADPH oxidase activity (42), further examination to elucidate the site of ROS generation related to Src activation in β-cells is needed. On the other hand, previous reports have shown that ROS itself regulates Src activity (43,44) in addition to Src activity regulation of ROS production (45). To clarify this mutual causal relationship between Src and ROS, we examined ROS production in GK islets expressing Src-KN, which was found to cause a distinct decrease in high-glucose–induced ROS production. This finding demonstrates that Src activity regulates ROS production and does not contradict the possibility of a feedback regulation mechanism of ROS on Src activity (45).

The high-glucose–induced increase in ATP production is impaired in GK rats (6,46) as well as in patients with type 2 diabetes (47). In addition, islets in GK rats and human type 2 diabetes are oxidatively stressed (48–50). In the present study, exendin-4 was able to recover this impaired increase in ATP production by high glucose in GK islets as well as to decrease excessive ROS production. Thus, GLP-1 signaling may improve β-cell function in the diabetic state not only because it enhances Ca^{2+} efficacy of the exocytotic system of insulin granules but also because it improves impaired metabolism-secretion coupling. GLP-1 receptor agonists are widely used in treatment of type 2 diabetes for their ability to improve glucose intolerance. Their clinical beneficial effect seems to be provided not only by their insulinotropic action but also by their reduction of β-cell apoptosis and induction of β-cell proliferation (16–18). Further elucidation of endogenous ROS regulation by GLP-1 may help to clarify the mechanism of the various beneficial effects of these agents.

ACKNOWLEDGMENTS

This work was supported by a research grant on Nanotechnical Medicine from the Ministry of Health, Labor, and Welfare of Japan; by scientific research grants from the Ministry of Education, Culture, Sports, Science, and Technology of Japan; and also by the Kyoto University Global Center of Excellence Program Center for Frontier Medicine.

No potential conflicts of interest relevant to this article were reported.

E.M. researched data, contributed to the discussion, wrote the manuscript, and reviewed/edited the manuscript. S.F. contributed to the discussion, wrote the manuscript, and reviewed/edited the manuscript. H.S., C.O., R.K., Y.S., M.S., and Y.N. researched data. M.O. contributed to the discussion and reviewed/edited the manuscript. N.I. contributed to the discussion and reviewed/edited the manuscript.

Parts of this study were presented in abstract form at the 70th Scientific Sessions of the American Diabetes Association, Orlando, Florida, 25–29 June 2010.

We acknowledge the editorial assistance of Dalmen Mayer. We thank C. Kotake for excellent technical assistance.

REFERENCES

1. Maechler P, Wollheim CB. Mitochondrial function in normal and diabetic beta-cells. Nature 2001;414:807–812
2. Krippeit-Drews P, Kramer C, Welker S, Lang F, Ammon HP, Drews G. Interference of H2O2 with stimulus-secretion coupling in mouse pancreatic beta-cells. J Physiol 1999;514(Pt 2):471–481
3. Maechler P, Jornot L, Wollheim CB. Hydrogen peroxide alters mitochondrial activation and insulin secretion in pancreatic beta cells. J Biol Chem 1999;274:27905–27913
4. Bindokas VP, Kuznetsov A, Sreenan S, Polonsky KS, Roe MW, Philipson LH. Visualizing superoxide production in normal and diabetic rat islets of Langerhans. J Biol Chem 2003;278:9796–9801
5. Sakai K, Matsumoto K, Nishikawa T, Suefuji M, Nakamaru K, Hirashima Y, Kawashima J, Shirotani T, Ichinose K, Brownlee M, Araki E. Mitochondrial reactive oxygen species reduce insulin secretion by pancreatic beta-cells. Biochem Biophys Res Commun 2003;300:216–222
6. Kominato R, Fujimoto S, Mukai E, Nakamura Y, Nabe K, Shimodahira M, Nishi Y, Funakoshi S, Seino Y, Inagaki N. Src activation generates reactive oxygen species and impairs metabolism-secretion coupling in diabetic Goto-Kakizaki and ouabain-treated rat pancreatic islets. Diabetologia 2008;51:1226–1235
7. Xu W, Harrison SC, Eck MJ. Three-dimensional structure of the tyrosine kinase c-Src. Nature 1997;385:595–602

8. Martin GS. The hunting of the Src. Nat Rev Mol Cell Biol 2001;2:467–475
9. Nada S, Okada M, MacAuley A, Cooper JA, Nakagawa H. Cloning of a complementary DNA for a protein-tyrosine kinase that specifically phosphorylates a negative regulatory site of p60c-src. Nature 1991;351: 69–72
10. Baggio LL, Drucker DJ. Biology of incretins: GLP-1 and GIP. Gastroenterology 2007;132:2131–2157
11. Holst JJ. The physiology of glucagon-like peptide 1. Physiol Rev 2007;87: 1409–1439
12. Seino S, Shibasaki T. PKA-dependent and PKA-independent pathways for cAMP-regulated exocytosis. Physiol Rev 2005;85:1303–1342
13. Roscioni SS, Elzinga CR, Schmidt M. Epac: effectors and biological functions. Naunyn Schmiedebergs Arch Pharmacol 2008;377:345–357
14. Ozaki N, Shibasaki T, Kashima Y, Miki T, Takahashi K, Ueno H, Sunaga Y, Yano H, Matsuura Y, Iwanaga T, Takai Y, Seino S. cAMP-GEFII is a direct target of cAMP in regulated exocytosis. Nat Cell Biol 2000;2:805–811
15. Kang G, Joseph JW, Chepurny OG, Monaco M, Wheeler MB, Bos JL, Schwede F, Genieser HG, Holz GG. Epac-selective cAMP analog 8-pCPT-2′-O-Me-cAMP as a stimulus for Ca2+-induced Ca2+ release and exocytosis in pancreatic beta-cells. J Biol Chem 2003;278:8279–8285
16. Xu G, Stoffers DA, Habener JF, Bonner-Weir S. Exendin-4 stimulates both β-cell replication and neogenesis, resulting in increased β-cell mass and improved glucose tolerance in diabetic rats. Diabetes 1999; 48:2270–2276
17. Farilla L, Hui H, Bertolotto C, Kang E, Bulotta A, Di Mario U, Perfetti R. Glucagon-like peptide-1 promotes islet cell growth and inhibits apoptosis in Zucker diabetic rats. Endocrinology 2002;143:4397–4408
18. Li Y, Hansotia T, Yusta B, Ris F, Halban PA, Drucker DJ. Glucagon-like peptide-1 receptor signaling modulates beta cell apoptosis. J Biol Chem 2003;278:471–478
19. Tsunekawa S, Yamamoto N, Tsukamoto K, Itoh Y, Kaneko Y, Kimura T, Ariyoshi Y, Miura Y, Oiso Y, Niki I. Protection of pancreatic beta-cells by exendin-4 may involve the reduction of endoplasmic reticulum stress; in vivo and in vitro studies. J Endocrinol 2007;193:65–74
20. Cheng Q, Law PK, de Gasparo M, Leung PS. Combination of the dipeptidyl peptidase IV inhibitor LAF237 [(S)-1-[(3-hydroxy-1-adamantyl)ammo]acetyl-2-cyanopyrrolidine] with the angiotensin II type 1 receptor antagonist valsartan [N-(1-oxopentyl)-N-[[2′-(1H-tetrazol-5-yl)-[1,1′-biphenyl]-4-yl]methyl]-L-valine] enhances pancreatic islet morphology and function in a mouse model of type 2 diabetes. J Pharmacol Exp Ther 2008;327:683–691
21. Akagi T, Sasai K, Hanafusa H. Refractory nature of normal human diploid fibroblasts with respect to oncogene-mediated transformation. Proc Natl Acad Sci U S A 2003;100:13567–13572
22. Florio M, Wilson LK, Trager JB, Thorner J, Martin GS. Aberrant protein phosphorylation at tyrosine is responsible for the growth-inhibitory action of pp60v-src expressed in the yeast Saccharomyces cerevisiae. Mol Biol Cell 1994;5:283–296
23. Mukai E, Fujimoto S, Sakurai F, Kawabata K, Yamashita M, Inagaki N, Mizuguchi H. Efficient gene transfer into murine pancreatic islets using adenovirus vectors. J Control Release 2007;119:136–141
24. Daub H, Weiss FU, Wallasch C, Ullrich A. Role of transactivation of the EGF receptor in signalling by G-protein-coupled receptors. Nature 1996; 379:557–560
25. Rozengurt E. Mitogenic signaling pathways induced by G protein-coupled receptors. J Cell Physiol 2007;213:589–602
26. Eguchi S, Iwasaki H, Inagami T, Numaguchi K, Yamakawa T, Motley ED, Owada KM, Marumo F, Hirata Y. Involvement of PYK2 in angiotensin II signaling of vascular smooth muscle cells. Hypertension 1999;33:201–206
27. Gao Y, Tang S, Zhou S, Ware JA. The thromboxane A2 receptor activates mitogen-activated protein kinase via protein kinase C-dependent Gi coupling and Src-dependent phosphorylation of the epidermal growth factor receptor. J Pharmacol Exp Ther 2001;296:426–433
28. Chiu T, Santiskulvong C, Rozengurt E. EGF receptor transactivation mediates ANG II-stimulated mitogenesis in intestinal epithelial cells through the PI3-kinase/Akt/mTOR/p70S6K1 signaling pathway. Am J Physiol Gastrointest Liver Physiol 2005;288:G182–G194
29. Harris KF, Shoji I, Cooper EM, Kumar S, Oda H, Howley PM. Ubiquitin-mediated degradation of active Src tyrosine kinase. Proc Natl Acad Sci U S A 1999;96:13738–13743
30. Yokouchi M, Kondo T, Sanjay A, Houghton A, Yoshimura A, Komiya S, Zhang H, Baron R. Src-catalyzed phosphorylation of c-Cbl leads to the interdependent ubiquitination of both proteins. J Biol Chem 2001;276: 35185–35193
31. Nada S, Yagi T, Takeda H, Tokunaga T, Nakagawa H, Ikawa Y, Okada M, Aizawa S. Constitutive activation of Src family kinases in mouse embryos that lack Csk. Cell 1993;73:1125–1135
32. Gates A, Hohenester S, Anwer MS, Webster CR. cAMP-GEF cytoprotection by Src tyrosine kinase activation of phosphoinositide-3-kinase p110 beta/alpha in rat hepatocytes. Am J Physiol Gastrointest Liver Physiol 2009;296: G764–G774
33. Buteau J, Foisy S, Joly E, Prentki M. Glucagon-like peptide 1 induces pancreatic β-cell proliferation via transactivation of the epidermal growth factor receptor. Diabetes 2003;52:124–132
34. Zhu QS, Xia L, Mills GB, Lowell CA, Touw IP, Corey SJ. G-CSF induced reactive oxygen species involves Lyn-PI3-kinase-Akt and contributes to myeloid cell growth. Blood 2006;107:1847–1856
35. Baumer AT, Ten Freyhaus H, Sauer H, Wartenberg M, Kappert K, Schnabel P, Konkol C, Hescheler J, Vantler M, Rosenkranz S. Phosphatidylinositol 3-kinase-dependent membrane recruitment of Rac-1 and p47phox is critical for alpha-platelet-derived growth factor receptor-induced production of reactive oxygen species. J Biol Chem 2008;283:7864–7876
36. Binker MG, Binker-Cosen AA, Richards D, Oliver B, Cosen-Binker LI. EGF promotes invasion by PANC-1 cells through Rac1/ROS-dependent secretion and activation of MMP-2. Biochem Biophys Res Commun 2009;379: 445–450
37. Peyot ML, Gray JP, Lamontagne J, Smith PJ, Holz GG, Madiraju SR, Prentki M, Heart E. Glucagon-like peptide-1 induced signaling and insulin secretion do not drive fuel and energy metabolism in primary rodent pancreatic beta-cells. PLoS One 2009;4:e6221
38. Tiedge M, Lortz S, Drinkgern J, Lenzen S. Relation between antioxidant enzyme gene expression and antioxidative defense status of insulin-producing cells. Diabetes 1997;46:1733–1742
39. Newsholme P, Haber EP, Hirabara SM, Rebelato EL, Procopio J, Morgan D, Oliveira-Emilio HC, Carpinelli AR, Curi R. Diabetes associated cell stress and dysfunction: role of mitochondrial and non-mitochondrial ROS production and activity. J Physiol 2007;583:9–24
40. Morgan D, Oliveira-Emilio HR, Keane D, Hirata AE, Santos da Rocha M, Bordin S, Curi R, Newsholme P, Carpinelli AR. Glucose, palmitate and pro-inflammatory cytokines modulate production and activity of a phagocyte-like NADPH oxidase in rat pancreatic islets and a clonal beta cell line. Diabetologia 2007;50:359–369
41. Nakayama M, Inoguchi T, Sonta T, Maeda Y, Sasaki S, Sawada F, Tsubouchi H, Sonoda N, Kobayashi K, Sumimoto H, Nawata H. Increased expression of NAD(P)H oxidase in islets of animal models of Type 2 diabetes and its improvement by an AT1 receptor antagonist. Biochem Biophys Res Commun 2005;332:927–933
42. Chowdhury AK, Watkins T, Parinandi NL, Saatian B, Kleinberg ME, Usatyuk PV, Natarajan V. Src-mediated tyrosine phosphorylation of p47phox in hyperoxia-induced activation of NADPH oxidase and generation of reactive oxygen species in lung endothelial cells. J Biol Chem 2005;280:20700–20711
43. Giannoni E, Buricchi F, Raugei G, Ramponi G, Chiarugi P. Intracellular reactive oxygen species activate Src tyrosine kinase during cell adhesion and anchorage-dependent cell growth. Mol Cell Biol 2005;25:6391–6403
44. Zhang J, Xing D, Gao X. Low-power laser irradiation activates Src tyrosine kinase through reactive oxygen species-mediated signaling pathway. J Cell Physiol 2008;217:518–528
45. Xie Z, Cai T. Na+-K+-ATPase-mediated signal transduction: from protein interaction to cellular function. Mol Interv 2003;3:157–168
46. Hughes SJ, Faehling M, Thorneley CW, Proks P, Ashcroft FM, Smith PA. Electrophysiological and metabolic characterization of single β-cells and islets from diabetic GK rats. Diabetes 1998;47:73–81
47. Anello M, Lupi R, Spampinato D, Piro S, Masini M, Boggi U, Del Prato S, Rabuazzo AM, Purrello F, Marchetti P. Functional and morphological alterations of mitochondria in pancreatic beta cells from type 2 diabetic patients. Diabetologia 2005;48:282–289
48. Ihara Y, Toyokuni S, Uchida K, Odaka H, Tanaka T, Ikeda H, Hiai H, Seino Y, Yamada Y. Hyperglycemia causes oxidative stress in pancreatic β-cells of GK rats, a model of type 2 diabetes. Diabetes 1999;48:927–932
49. Sakuraba H, Mizukami H, Yagihashi N, Wada R, Hanyu C, Yagihashi S. Reduced beta-cell mass and expression of oxidative stress-related DNA damage in the islet of Japanese Type II diabetic patients. Diabetologia 2002;45:85–96
50. Del Guerra S, Lupi R, Marselli L, Masini M, Bugliani M, Sbrana S, Torri S, Pollera M, Boggi U, Mosca F, Del Prato S, Marchetti P. Functional and molecular defects of pancreatic islets in human type 2 diabetes. Diabetes 2005;54:727–735

Pediatric Diabetes

ISPAD International Society for Pediatric and Adolescent Diabetes

Pediatric Diabetes 2012: 13: 26–32
doi: 10.1111/j.1399-5448.2011.00827.x

Pediatric Diabetes

Original Article

Comprehensive molecular analysis of Japanese patients with pediatric-onset MODY-type diabetes mellitus

Yorifuji T, Fujimaru R, Hosokawa Y, Tamagawa N, Shiozaki M, Aizu K, Jinno K, Maruo Y, Nagasaka H, Tajima T, Kobayashi K, Urakami T. Comprehensive molecular analysis of Japanese patients with pediatric-onset MODY-type diabetes mellitus.
Pediatric Diabetes 2012: 13: 26–32.

Background: In Asians, mutations in the known maturity-onset diabetes of the young (MODY) genes have been identified in only <15% of patients. These results were obtained mostly through studies on adult patients.
Objective: To investigate the molecular basis of Japanese patients with pediatric-onset MODY-type diabetes.
Subjects: Eighty Japanese patients with pediatric-onset MODY-type diabetes.
Methods: Mitochondrial 3243A>G mutation was first tested by the polymerase chain reaction restriction fragment length polymorphism analysis for maternally inherited families. Then, all coding exons and exon–intron boundaries of the *HNF1A*, *HNF1B*, *GCK*, and *HNF4A* genes were amplified from genomic DNA and directly sequenced. Multiplex ligation-dependent probe amplification analysis was also performed to detect whole-exon deletions.
Results: After excluding one patient with a mitochondrial 3243A>G, mutations were identified in 38 (48.1%) patients; 18 had *GCK* mutations, 11 had *HNF1A* mutations, 3 had *HNF4A* mutations, and 6 had *HNF1B* mutations. In patients aged <8 yr, mutations were detected mostly in *GCK* at a higher frequency (63.6%). In patients >9 yr of age, mutations were identified less frequently (45.1%), with *HNF1A* mutations being the most frequent. A large fraction of mutation-negative patients showed elevated homeostasis model assessment (HOMA) insulin-resistance and normal HOMA-β indices. Most of the *HNF1B* mutations were large deletions, and, interestingly, renal cysts were undetectable in two patients with whole-gene deletion of *HNF1B*.
Conclusion: In Japanese patients with pediatric-onset MODY-type diabetes, mutations in known genes were identified at a much higher frequency than previously reported for adult Asians. A fraction of mutation-negative patients presented with insulin-resistance and normal insulin-secretory capacities resembling early-onset type 2 diabetes.

Tohru Yorifuji[a,b], Rika Fujimaru[a], Yuki Hosokawa[a], Nobuyoshi Tamagawa[b], Momoko Shiozaki[b], Katsuya Aizu[c], Kazuhiko Jinno[d], Yoshihiro Maruo[e], Hironori Nagasaka[f], Toshihiro Tajima[g], Koji Kobayashi[h] and Tatsuhiko Urakami[i]

[a]Department of Pediatric Endocrinology and Metabolism, Children's Medical Center, Osaka City General Hospital, 2-13-22 Miyakojima-Hondori, Miyakojima, Osaka 534-0021, Japan; [b]Clinical Research Center, Osaka City General Hospital, 5-15-21 Nakano, Miyakojima, Osaka 534-0027, Japan; [c]Division of Endocrinology and Metabolism, Saitama Children's Medical Center, 2100 Magome, Iwatsuki, Saitama 339-8551, Japan; [d]Department of Pediatrics, Hiroshima General Hospital of West Japan Railway Company, 3-1-36 Futabanosato, Higashi, Hiroshima 732-0057, Japan; [e]Department of Pediatrics, Shiga University of Medical Science, Seta-Tsukinowa, Otsu, Shiga 520-2192, Japan; [f]Department of Pediatrics, Takarazuka City Hospital, 4-5-1 Obama, Takarazuka, Hyogo 665-0827, Japan; [g]Department of Pediatrics, Hokkaido University School of Medicine, Kita 14, Nishi 5, Kita, Sapporo 060-8648, Japan; [h]Department of Pediatrics, Yamanashi Kosei Hospital, 860 Ochiai, Yamanashi, Yamanashi 405-0033, Japan; and [i]Department of Pediatrics, Nihon University School of Medicine, 1-8-13 Kanda Surugadai, Chiyoda, Tokyo 101-8309, Japan

Key words: Japanese – MODY – mutation – pediatric

Corresponding author:
Tohru Yorifuji, MD, PhD, Department of Pediatric Endocrinology and Metabolism, Children's Medical Center, Osaka City General Hospital, 2-13-22 Miyakojima-Hondori, Miyakojima, Osaka 534-0021, Japan.
Tel: +81 6 6929 1221;
fax: +81 6 6929 1090;
e-mail: yorif@kuhp.kyoto-u.ac.jp

Submitted 30 August 2011.
Accepted for publication 15 September 2011

Maturity-onset diabetes of the young (MODY) has been defined as diabetes mellitus characterized by dominant inheritance, non-obesity [body mass index (BMI) <25], and early onset (<25 years of age). To date, at least six causative genes (*HNF4A, GCK, HNF1A, PDX1, HNF1B,* and *NEUROD1*) for MODY 1–6, respectively, have been identified. In addition, several other genes (*KLF11, CEL, PAX4*, and *INS*) have been shown to be associated with MODY-type diabetes (1–6). Since the term 'MODY' has been questioned by some investigators as inappropriate and obsolete (1), 'MODY-type diabetes' is used in this study to describe diabetes with above characteristics.

Previous studies have revealed that mutations in these genes, especially in the *HNF1A*, *GCK*, and *HNF4A* genes, account for 54–86% of MODY-type diabetes in Caucasians, whereas in Asians, only 7.5–10.3% of patients have mutations in these genes (7–13). In the Japanese, previous studies have focused mainly on single genes (14–16), and comprehensive molecular analysis is lacking. Taken together, however, these studies point to a similarly low prevalence of mutations (<15%) in the Japanese.

One possible explanation for this racial disparity is the presence of an unidentified major MODY-X gene in Asians. To date, a number of investigators have pursued this possibility without much success, only to identify genes with low prevalence (17–23). Alternatively, this racial difference could be due to the higher prevalence of early-onset type 2 diabetes mellitus (T2DM) in Asians (24). Japanese patients with T2DM reportedly have lower body mass indices (BMIs) than do Caucasian patients (25). Although, T2DM is based on insulin-resistance rather than on ?-cell dysfunction, clinical differentiation between these is not easy when the patients are not obese and the onset of diabetes is earlier, because both tend to aggregate within families and are autoantibody negative.

In this study, as part of an effort to address this issue, we performed a comprehensive mutational analysis on Japanese patients with pediatric-onset MODY-type diabetes mellitus because previous results were obtained mostly through studies on adult patients. This is also the most comprehensive molecular analysis of known MODY genes in Japan. Unexpectedly, our study revealed that the genetic background of MODY-type diabetes in the Japanese pediatric age group is similar to that reported for Caucasians. The results of this study, therefore, served to delineate the demographic and clinical characteristics of 'unknown MODY' in the Japanese.

Subjects and methods

Subjects

The study subjects were 80 Japanese patients who developed MODY-type diabetes before 20 yr of age. Other inclusion criteria were (i) negative autoantibodies, including anti-GAD and anti-IA2 antibodies; (ii) family history suggestive of dominant inheritance; and (iii) non-obesity in the patients or in affected family members. Patients who developed diabetes before 6 months of age were excluded because the genetic background of diabetes in this age group is known to differ from those in later age groups (26). In addition to the 77 patients who met the above criteria, 3 additional patients without a positive family history were included because of the known presence of renal cysts.

Out of these 80 patients, 56 were ascertained through the nationwide school urinalysis program performed annually in Japan, and 21 by incidentally identified glucosuria/hyperglycemia. The rest of the patients were ascertained after consulting primary care physicians for diabetes-related symptoms. The patients were then referred to local diabetes centers and blood samples were sent to our laboratory during 2005–2011 under a suspected diagnosis of MODY-type diabetes. The local diabetes centers were distributed throughout Japan without geographical biases and each center basically recruited all available patients for analysis.

The patients were enrolled after obtaining written informed consent, and the study protocol was approved

by the Institutional Review Board at Osaka City General Hospital (No. 742).

Mutational analysis

Genomic DNA was extracted from peripheral blood leukocytes with the QIAamp DNA Blood Kit (QIAGEN, Hilden, Germany). In families with maternal transmission, the mitochondrial 3243A>G mutation was first tested by polymerase chain reaction (PCR)-restriction fragment length polymorphism as previously described (27). For patients negative for 3243A>G, all coding exons, exon–intron boundaries, and promoter regions of the *HNF1A*, *GCK*, *HNF4A*, and *HNF1B* genes were amplified from genomic DNA. For *HNF4A*, exon 1D and the P2 promoter approximately 50 kb upstream of exon 1A were also amplified because previous reports identified this region as a specific promoter for pancreatic expression of this gene (28). For *GCK*, the pancreatic form using exon 1A was sequenced (29). The primer sequences and amplification conditions are listed in Table S1 and Appendix S1. The amplified products were purified using the Wizard PCR Preps DNA Purification Kit (Promega, Madison, WI, USA) or the Agencourt AMPure XP purification system (Beckman Coulter Genomics, Danvers, MA, USA) and directly sequenced using the BIGDYE TERMINATOR v3.1 Cycle Sequencing Kit (Roche, Basel, Switzerland). They were then analyzed by the ABI PRISM 3100xl automated sequencer (Applied Biosystems, Foster City, CA, USA). After identification, co-segregation of the mutations with the diabetic phenotype was confirmed by sequencing analyses of other family members. In addition, whole-exon deletion/duplications that might escape the PCR-sequencing strategy described above were tested using multiplex ligation-dependent probe amplification (MLPA) analyses. Briefly, 200 ng of genomic DNA was used to perform the MLPA reactions for all exons in the *HNF1A*, *GCK*, *HNF4A*, and *HNF1B* genes. The reactions were performed using the SALSA MLPA kit P241 (MRC-Holland, Amsterdam, The Netherlands) as recommended by the manufacturer and analyzed using the ABI PRISM 3100xl automated sequencer and GENEMAPPER software (Applied Biosystems).

Results

Mitochondrial 3243A>G was found in one patient and the patient was excluded from further analysis. Of the remaining 79 patients, mutations were identified in 38 (48.1%), which is a much higher frequency than that previously reported for Asians. The demographic and clinical features of these 38 patients are listed in Table 1 together with the details of identified mutations.

Mutations of *HNF1A* were identified in 11, *GCK* in 18, *HNF4A* in 3, and *HNF1B* in 6 (Table 1). Most of these mutations have been previously reported, and no predominant mutation was identified. Novel missense mutations were not found in the public domain single nucleotide polymorphism databases, and the Sorting Intolerant from Tolerant (SIFT) (http://sift.bii.a-star.edu.sg/) or the POLYPHEN-2 (http://genetics.bwh.harvard.edu/pph2/) programs predicted the deleterious nature of these mutations. In addition, these mutations co-segregated with the diabetic phenotype in each family, suggesting that these are pathogenic mutations.

The majority of patients (five out of six) with *HNF1B* mutations had exon deletions. All these patients with deletions presented with a higher blood glucose level at onset, necessitating immediate insulin treatment. Interestingly, in two patients with whole-gene deletion (patients 32 and 34), renal cysts could not be identified by repeated abdominal magnetic resonance imaging or echography.

We also identified a whole-gene deletion of the *GCK* gene in one patient (patient 15). This patient was born after 39 weeks of gestation with a birth weight of 2418 g. Hyperglycemia was incidentally found at the age of 4 years, and the patient showed no diabetes-related symptoms. Fasting glucose and hemoglobin A1c were slightly elevated at 124 mg/dL (6.88 mmol/L) and 6.6%, respectively. All of these features were consistent with those of other GCK-MODY patients, and no specific features were observed for this patient.

When the patients were sorted by age at diagnosis (Fig. 1), *GCK* mutations were found to be predominant in patients <9 years of age, whereas detection of mutations in the *HNF1A* and *HNF4A* genes began after 8 years of age. After 9 years of age, *HNF1A* mutations were the most common. The frequency and spectrum of mutations did not change significantly during 9–13 years of age, and the identification rate appeared to decline thereafter.

BMI percentiles at diagnosis were obtained for 76 patients. For patients who lost weight before the initial presentation, the most recent height and weight data before weight loss were used for the calculation of BMI. Mutations were identified in 89% of the leanest patients with BMIs below the 10th percentile (Fig. 2). Between BMIs of the 10th–90th percentiles, mutations were identified at a relatively constant frequency, although the detection rate appeared to be lower (10%) for BMIs above the 90th percentile.

The homeostasis model assessment insulin-resistance (HOMA-IR) index as a marker of insulin resistance (normal range, <2.0) and the HOMA-β index as a marker of insulin-secreting capacity (normal range for Japanese, 40–60) were calculated for 57 patients (30). As shown in Table 2, a large

Table 1. Summary of patients with mutations

No.	Gene	Mutation		Previous report	Gender	Age (yr)	BMI per-centile	FBS, mg/dL (mmol/L)	IRI, μU/mL (pmol/L)	HOMA-IR	HOMA-β
		cDNA	Protein								
1	*GCK*	c.1517C>T	p.T206M	Yes	F	3	95.2	82 (4.55)	1.5 (10.42)	0.30	28.4
2	*GCK*	c.130G>A	p.G44S	Yes	M	5	83.48	118 (6.55)	2.8 (19.45)	0.81	18.3
3	*GCK*	c.571C>T	p.R191W	Yes	M	11	80.45	144 (7.99)	20.4 (141.68)	7.25	90.7
4	*GCK*	c.1278_1286dup9	p.S426_R428dup	No	M	6	76.17	120 (6.66)	4.16 (28.89)	1.37	29.1
5	*GCK*	c.895G>C	p.G299R	Yes	M	9	58.08	122 (6.77)	4.6 (31.95)	1.39	28.1
6	*GCK*	c.1142T>G	p.M381R	No	M	14	57.13	139 (7.71)	5.8 (40.28)	1.99	27.5
7	*GCK*	c.571C>T	p.R191W	Yes	M	7	40.63	124 (6.88)	5.5 (38.2)	1.68	32.5
8	*GCK*	c.175C>T	p.P59S	No	M	5	32.61	118 (6.55)	2 (13.89)	0.58	13.1
9	*GCK*	c.781G>A	p.G261R	Yes	M	4	24.88	106 (5.88)	1.54 (10.7)	0.40	12.9
10	*GCK*	c.118G>A	p.E40K	Yes	M	1	23.18	129 (7.16)	2 (13.89)	0.64	10.9
11	*GCK*	c.575G>A	p.R191Q	Yes	M	5	21.5	118 (6.55)	7.1 (49.31)	2.07	46.5
12	*GCK*	c.182A>G	p.Y61C	No	F	8	20.52	118 (6.55)	1.82 (12.64)	0.53	11.9
13	*GCK*	c.234C>G	p.D38E	Yes	F	13	12.8	121 (6.72)	5.73 (39.79)	1.71	35.6
14	*GCK*	c.556C>T	p.R186X	Yes	F	12	11.52	135 (7.49)	10.3 (71.53)	3.43	51.5
15	*GCK*	All exon deletion		No	M	4	6.68	124 (6.88	3.42 (23.75)	1.05	20.2
16	*GCK*	c.437T>G	p.L146R	Yes	M	8	5.07	119 (6.6)	2.3 (15.97)	0.68	14.8
17	*GCK*	c.576G>T	p.G193W	No	M	12	1.92	118 (6.55)	6.36 (44.17)	1.85	41.6
18	*GCK*	c.500G>A	p.W167X	No	F	5	0.43	113 (6.27)	4 (27.78)	1.12	28.8
19	*HNF1A*	c.1043T>C	p.L348P	No	F	15	83.1	175 (9.71)	21.6 (150.01)	9.33	69.4
20	*HNF1A*	c.779C>T	p.T260M	Yes	F	12	80.53	124 (6.88)	10.6 (73.62)	3.25	62.6
21	*HNF1A*	c.391C>T	p.R131W	Yes	M	9	78.79	124 (6.88)	5.37 (37.29)	1.64	31.7
22	*HNF1A*	Exon 7-9 deletion		No	M	11	68.07	165 (9.16)	11.4 (79.17)	4.6	40.2
23	*HNF1A*	c.788G>A	p.R263H	Yes	M	8	48.33	84 (4.66)	3.29 (22.85)	0.68	56.4
24	*HNF1A*	c.872delC	p.P291fs	Yes	M	13	43.38	83 (4.61)	11.3 (78.48)	2.32	203.4
25	*HNF1A*	c.1181delC	p.P394fs	Yes	F	13	21.83	137 (7.6)	7.3 (50.7)	2.47	35.5
26	*HNF1A*	c.1054delT	p.S352fs	No	F	11	18.66	153 (8.49)	2.7 (18.75)	1.02	10.8
27	*HNF1A*	c.392G>A	p.R131Q	Yes	F	11	2.0	167 (9.27)	7.9 (54.87)	3.26	27.3
28	*HNF1A*	c.872_873insC	p.P291fs	Yes	F	13	1.65	98 (5.44)	7.18 (49.87)	1.74	73.9
29	*HNF1A*	c.598C>T	p.R200W	Yes	M	14	0.33	77 (4.27)	0.9 (6.25)	0.17	23.1
30	*HNF1B*	c.395A>C	p.H132P	No	M	7	70	111 (6.16)	10.3 (71.53)	2.82	77.3
31	*HNF1B*	Exon 1-4 deletion		No	M	1	62.16	NA	NA	NA	NA
32	*HNF1B*	All exon deletion		Yes	F	13	38.68	NA	NA	NA	NA
33	*HNF1B*	Exon 3-4 deletion		No	M	12	19.23	NA	NA	NA	NA
34	*HNF1B*	All exon deletion		Yes	F	12	8.42	NA	NA	NA	NA
35	*HNF1B*	Exon 3-4 deletion		No	F	10	NA	NA	NA	NA	NA
36	*HNF4A*	c.802C>T	p.Q268X	Yes	F	9	77.22	NA	NA	NA	NA
37	*HNF4A*	c.915_916insT	p.V306fs	No	F	11	55.28	105 (5.83)	7.2 (50)	1.87	61.7
38	*HNF4A*	c.970C>T	p.R324C	No	F	13	45.36	188 (10.43)	6.5 (45.14)	3.02	18.7

BMI, body mass index; F, female; FBS, fasting blood sugar; HOMA-β, homeostasis model assessment-β; HOMA-IR, homeostasis model assessment insulin resistance; IRI, immunoreactive insulin; M, male; NA, not available.

All sequence information is based on GenBank reference sequences NM_000162.3 (*GCK*), NM_000457.3 (*HNF4A*), NM_000545.5 (*HNF1A*), and NM_000458.2 (*HNF1B*). Nucleotide numbering reflects cDNA numbering with +1 corresponding to the A of the major start codon of exon 1 (*HNF1A* and *HNF1B*) and 1A (*GCK*), respectively. For *HNF4A*, conventional nucleotide numbering starting at the A of the Met9 of isoform b was used.

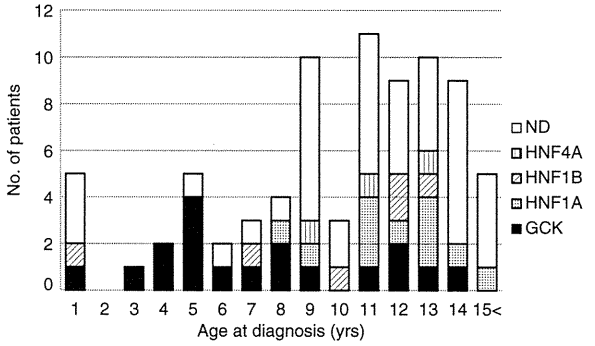

Fig. 1. Distribution of age at diagnosis. ND, not detected.

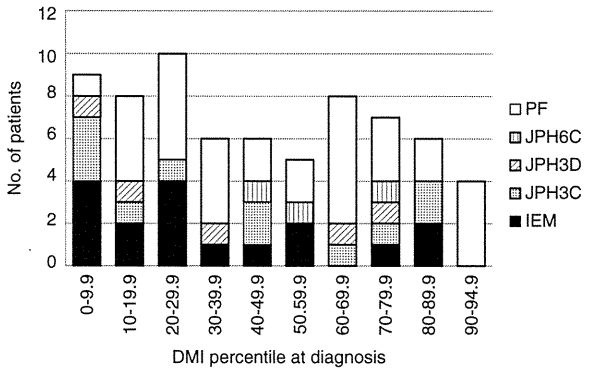

Fig. 2. Distribution of body mass index percentiles at diagnosis. ND, not detected.

fraction of mutation-negative patients showed elevated HOMA-IR or normal HOMA-β indices. Mutations were identified less frequently with increasing HOMA-IR or HOMA-β indices ($p = 0.0248$ and 0.002, respectively, by the Jonckheere's trend test). In the remaining 22 patients, these indices were not available because of the lack of fasting glucose and insulin data at diagnosis. Nineteen of these patients presented with a blood glucose level that was too high (>170 mg/dL, 9.44 mmol/L) at diagnosis to calculate these indices, and/or insulin therapy was initiated immediately before calculating these indices. In three patients, fasting glucose and insulin data were not recorded or simply not obtained. Of these 22 patients with missing HOMA-IR and HOMA-β data, mutations were identified in 6 (27.3%); 4 had *HNF1B* mutations and 2 had *HNF4A* mutations.

Discussion

Contrary to previous studies on Asians, the results of this study showed that the frequency of mutations in known genes is significantly higher in pediatric-onset Japanese patients with MODY-type diabetes. Even if we exclude the three patients with renal cysts and without positive family history, the mutation identification rate (46.1%) was still higher than previously reported. The overall frequency of mutation was only slightly lower than that reported for Caucasians (7–11), and the mutation spectrum did not differ much between Japanese and Caucasian patients. These results suggest that the genetic background of MODY-type diabetes in the pediatric age group is similar for these two ethnicities.

The cause of the difference in the frequencies of mutations between adult Asian and Caucasian MODY patients remains unclear. Assuming that the genetic background of pediatric-onset patients is similar, the racial disparity should be caused by a group of patients who develop diabetes at a later age (15–25 yr).

Among pediatric-onset patients, mutation-negative patients are likely to comprise a mixed population. There is a group of patients who fit the classical definition of MODY with normal insulin sensitivity and diminished insulin-secretory capacity. Presumably, some of these patients' conditions can be explained by mutations in the known MODY genes, including *PAX4* and *INS*, and the remaining was caused by mutations in true MODY-X genes. At present, there is no evidence of racial disparity in this group of patients.

The results of our study also showed that a large fraction of mutation-negative patients has elevated insulin-resistance and normal insulin-secretory capacities as measured by the HOMA-IR and HOMA-β indices. Although these patients' conditions might also be explained by an unknown monogenic trait, these clinical features are more consistent with those of early-onset T2DM, which is highly prevalent in Japan. Considering the known racial difference in the incidence of T2DM, the observed difference in the

Table 2. Distribution of HOMA-IR and HOMA-β indices

	HOMA-IR			HOMA-β					
	0–0.99	1–1.99	>2	10–19.9	20–29.9	30–39.9	40–49.9	50–59.9	>60
No. of patients	15	20	22	9	12	7	6	6	17
Mutation positive	10	12	10	7	8	4	3	3	7
Fraction mutation positive	0.67	0.6	0.45	0.78	0.67	0.57	0.5	0.5	0.41

HOMA-β, homeostasis model assessment-β; HOMA-IR, homeostasis model assessment insulin resistance.
HOMA-IR was calculated as fasting blood glucose (mg/dL) × fasting insulin (μU/mL)/405 (normal range, <2.0), and HOMA-β was calculated as 360 × fasting insulin (μU/mL)/fasting blood glucose (mg/dL) − 63 (normal range for Japanese, 40–60).

prevalence of MODY gene mutations in adult patients appears to be more easily explained by inclusion of early-onset T2DM in previous studies. Although adult T2DM patients in Japan are not heavier than non-diabetic controls (25), even in Japan, pediatric patients with T2DM are heavier than their peers (31). By focusing on non-obese pediatric patients, we may be able to minimize the influence of early-onset T2DM in our study. A similar explanation might also apply to other ethnic groups, such as Mexicans, known to have a higher prevalence of T2DM and lower prevalence of MODY gene mutations (32).

As previously reported for pediatric patients with *HNF1B* mutations, the majority of our HNF1B-MODY patients had deletions rather than point mutations (33, 34). This is in contrast to the approximately 30% prevalence of deletions in adult patients (35). It was previously proposed that deletions might lead to more severe loss of function, which leads to earlier onset of diabetes (34). In our series, patients with *HNF1B* deletions (patients 31–35) actually presented with higher blood glucose at onset compared with patient 30, who had a point mutation. It appears more likely, however, that interactions with other genetic or environmental factors play a more important role in determination of the phenotype of *HNF1B* mutations because none of the deletion patients reported by Ulinski et al. (33) had diabetes, and some patients with a whole-gene deletion do not have renal structural abnormalities (34), including the two patients in our series. Practically, it is important to include the analysis of *HNF1B* deletions as a part of routine mutation screening of MODY-type diabetes, even without signs of renal abnormalities.

Acknowledgements

We thank the patients and their families for participating in our research. We also thank pediatric endocrinologists and diabetologists across Japan who referred their patients to us. This work was supported in part by a Grant-in-Aid for Scientific Research (Research on Measures for Intractable Diseases) from the Ministry of Health, Labour and Welfare of Japan.

Conflict of interest

No conflict of interests declared.

Supporting Information

Additional Supporting Information may be found in the online version of this article:

Appendix S1. Amplification conditions.

Table S1. Sequences of the primers used for amplification.

Please note: Wiley-Blackwell are not responsible for the content or functionality of any supporting materials supplied by the authors. Any queries (other than missing material) should be directed to the corresponding author for the article.

References

1. Murphy R, Ellard S, Hattersley A. Clinical implications of a molecular genetic classification of monogenic β-cell diabetes. Nat Clin Pract Endocrinol Metab 2008: 4: 200–213.
2. Vaxillaire M, Froguel P. Monogenic diabetes in the young, pharmacogenetics and relevance to multifactorial forms of type 2 diabetes. Endocr Rev 2008: 29: 254–264.
3. Neve B, Fernandez-Zapico ME, Ashkenazi-Katalan V et al. Role of transcription factor KLF11 and its diabetes-associated gene variants in pancreatic beta cell function. Proc Natl Acad Sci U S A 2005: 102: 4807–4812.
4. Raeder H, Johansson S, Holm PI et al. Mutations in the CEL VNTR cause a syndrome of diabetes and pancreatic exocrine dysfunction. Nat Genet 2006: 38: 54–62.
5. Shimajiri Y, Sanke T, Furuta H Y et al. A missense mutation of Pax4 gene (R121W) is associated with type 2 diabetes in Japanese. Diabetes 2001: 50: 2864–2869.
6. Molven A, Ringdal M, Nordbø AM et al. Mutations in the insulin gene can cause MODY and autoantibody-negative type 1 diabetes. Diabetes 2008: 57: 1131–1135.
7. Frayling TM, Evans JC, Bulman MP et al. Beta-cell genes and diabetes: molecular and clinical characterization of mutations in transcription factors. Diabetes 2001: 50 (Suppl. 1): S94–S100.
8. Froguel P, Zouali H, Vionnet N et al. Familial hyperglycemia due to mutations in glucokinase. Definition of a subtype of diabetes mellitus. N Engl J Med 1993: 328: 697–702.
9. Lindner TH, Cockburn BN, Bell GI. Molecular genetics of MODY in Germany. Diabetologia 1999: 42: 121–123.
10. Letho M, Wipemo C, Ivarsson SA et al. High frequency of mutations in MODY and mitochondrial genes in Scandinavian patients with familial early-onset diabetes. Diabetologia 1999: 42: 1131–1137.
11. Costa A, Bescos M, Velho G et al. Genetic and clinical characterization of maturity-onset diabetes of the young in Spanish families. Eur J Endocrinol 2000: 142: 380–386.
12. Hwang JS, Shin CH, Yang SW, Jung SY, Huh N. Genetic and clinical of Korean maturity-onset diabetes of the young (MODY) patients. Diabetes Res Clin Pract 2006: 74: 75–81.
13. Ng MC, Cockburn BN, Lindner TH et al. Molecular genetics of diabetes mellitus in Chinese subjects: identification of mutations in glucokinase and hepatocyte nuclear factor-1 alpha genes in patients with early-onset type 2 diabetes mellitus/MODY. Diabet Med 1999: 16: 956–963.
14. Tonooka N, Tomura H, Takahashi Y et al. High frequency of mutations in the HNF-1α gene (TCF1) in non-obese patients with diabetes of youth in Japanese and identification of a case of digenic inheritance. Diabetologia 2002: 45: 1709–1712.